ELSEVIER

Journal of Atmospheric and Solar-Terrestrial Physics 69 (2007) 2309–2337

Journal of ATMOSPHERIC AND SOLAR-TERRESTRIAL PHYSICS

www.elsevier.com/locate/jastp

Stratospheric warming effects on the tropical mesospheric temperature field

M.G. Shepherd[a,*], D.L. Wu[b], I.N. Fedulina[c], S. Gurubaran[d], J.M. Russell[e], M.G. Mlynczak[f], G.G. Shepherd[a]

[a]*Centre for Research in Earth and Space Science, York University, 4700 Keele Street, Toronto Ont., Canada M3J 1P3*
[b]*Microwave Atmos. Sc., M/S 183-701, 4800 Oak Grove Dr., JPL/Caltech, Pasadena, CA 91109, USA*
[c]*Institute of Ionosphere, Kamenskoe Plato, Almaty 480020, Kazakhstan*
[d]*Equatorial Geophysical Research Laboratory, Indian Institute of Geomagnetism Krishnapuram, Tirunelveli 627 011, India*
[e]*Hampton University, Hampton, VA, USA*
[f]*NASA Langley Research Center, Hampton, VA, USA*

Received 30 January 2007; received in revised form 12 April 2007; accepted 25 April 2007
Available online 6 May 2007

Abstract

Temperature observations at 20–90 km height and 5–15°N during the winter of 1992–1993, 1993–1994 and 2003–2004, from the Wind Imaging Interferometer (WINDII) and Microwave Limb Sounder (MLS) experiments on the Upper Atmosphere Research Satellite (UARS) satellite and the Sounding the Atmosphere using Broadband Emission Radiometry (SABER) experiment on the Thermosphere, Ionosphere, Mesosphere Energetics and Dynamics (TIMED) satellite are analyzed together with MF radar winds and UK Meteorological Office (UKMO) assimilated fields. Mesospheric cooling is observed at the time of stratospheric warming at the tropics correlative with stratospheric warming events at middle and high latitudes. Planetary waves $m = 1$ with periods of 4–5, 6–8, 10 and 12–18 days are found to dominate the period. Westward 7- and 16-day waves at the tropics appear enhanced by stationary planetary waves during sudden stratospheric warming events.

Keywords: Tropical mesosphere; Temperature; Stratospheric warming; Satellites

1. Introduction

While extensive studies have been conducted on the effects of sudden stratospheric warmings (SSW) on the upper mesosphere and the MLT region at high and mid-latitudes (e.g. Whiteway and Carswell, 1994; Walterscheid et al., 2000; Hoffman et al., 2002; Manson et al., 2006), there are only few reports on the possible effect of SSW on the tropical middle atmosphere and the coupling between the tropical and high-latitude middle atmospheres during such events (Fritz and Soules, 1970; Mukherjee and Ramana Murty, 1972; Mukherjee et al., 1987; Sivakumar et al., 2004; Kodera, 2006). Using observations from the Nimbus 3 satellite, Fritz and Soules (1970) were the first to show that the perturbations in the stratosphere at the higher latitudes are related to those at the tropics: the

*Corresponding author. Tel.: +1 416 7362100; fax: +1 416 7365626.
E-mail address: mshepher@yorku.ca (M.G. Shepherd).

1364-6826/$ - see front matter © 2007 Elsevier Ltd. All rights reserved.
doi:10.1016/j.jastp.2007.04.009

SSW at high latitudes in winter were accompanied by simultaneous cooling in the tropical winter stratosphere and in the summer hemisphere.[1]

Mukherjee and Ramana Murty (1972) examined the effects of possible SSW on the middle atmosphere using rocket-sonde data from Thumba (8.5°N, 76°E) from December 1970 to March 1971 and found that occasional warmings do occur at these latitudes in the upper stratosphere and mesosphere, consistent with the observations of intense mesospheric cooling at high latitudes (Quiroz, 1969; Labitzke, 1972; Gregory and Manson, 1975; Hirota and Barnett, 1977; Mirabø et al., 1984; Delisi and Dunkerton, 1988). More recently, such intense mesospheric cooling was also reported by Walterscheid et al. (2000) and Cho et al. (2004), and was found to be closely associated, but preceding in time the warming in the stratosphere.

Mukherjee et al. (1987) also examined the dynamics of the tropical stratosphere and mesosphere in the winter of 1984–1985 employing weekly rocket temperature profiles and radar winds at Thumba (9°N) The period was marked by a minor stratospheric warming followed by a major stratospheric warming event registered at high latitudes. At the tropical lower mesosphere, deep cold and warm temperature anomalies[2] were observed prior to the major stratospheric warming, which was observed about 2 weeks later, accompanied by a cold anomaly in the mesosphere. The zonal winds were strong easterlies[3] in the upper stratosphere and the lower mesosphere.

In a recent study, Sivakumar et al. (2004) also examined the stratospheric warming effects at low latitudes employing Rayleigh lidar temperature observations from Gadanki (13.5°N, 79.2°E). They reported a stratospheric warming event at low latitudes about a week after a major stratospheric warming was registered at high latitudes, with a temperature increase of ~18 K above the tropical winter mean values at 45 km height.

It is well established now that the coupling between high and tropical latitudes is not restricted only to stratospheric warming effects. Signatures of such equatorial and low-latitude phenomenon as the quasi-biennial oscillation (QBO) have also been observed at middle and high latitudes (e.g. Gray et al., 2001 and references therein). It has been suggested that the QBO can trigger the stratospheric warming events (Labitzke, 1987) (for more on QBO, please see Baldwin et al., 2001). Labitzke (1987) investigated inter-annual variability of the SSW and showed that more major stratospheric mid-winter SSW occurred in the easterly phase of the stratospheric QBO (westerly phase of the mesospheric QBO) and that the relatively few major mid-winter SSW observed in the westerly phase of the QBO took place only when the sunspot number was high. These results suggest that the QBO influences the cooling in the polar MLT region associated with the SSW.

While most of the reports concerning the state of the winter tropical middle atmosphere (stratosphere and mesosphere) are based on ground-based and rocket observations from the Indian subcontinent, satellite missions like the Upper Atmosphere Research Satellite (UARS) (Reber et al., 1993), and the Thermosphere, Ionosphere, Mesosphere Energetics and Dynamics (TIMED) (Yee, 2003) provide the opportunity to investigate the state of the tropical middle atmosphere on a global scale.

Here we report the results from the analysis of satellite temperature observations from the Wind Imaging Interferometer (WINDII) (Shepherd et al., 1993), the Microwave Limb Sounder (MLS) experiments on UARS and the Sounding the Atmosphere using Broadband Emission Radiometry (SABER) (Mlynczak, 1997; Russell et al., 1999) experiment on TIMED, combined with ground-based MF radar (c) zonal and meridional winds from Tirunelveli (8.7°N, 77.8°E). The UK Meteorological Office (UKMO) assimilated temperature and winds data have also been considered. The MFR winds data are obtained at a site very close to those used in the work of Mukherjee and Ramana Murty (1972), Mukherjee et al. (1987) and Sivakumar et al. (2004), and together with satellite observations in the same 5–15°N latitude range allow parallels to be drawn to those earlier reports in the interpretation and discussion of our results.

Manney et al. (2005) examined stratospheric zonal mean wind data from 26 Arctic winters, from 1978 to 2004 and showed that the period from 1989 to 1998 did not have any major SSW, while there were seven major SSW in the period from December 1998 to April 2004. Thus we will examine the possible effects on the tropical mesosphere by minor SSW employing temperature and wind observations

[1]For more on stratospheric sudden warmings, please see Andrews et al. (1987).

[2]Temperature anomaly is a deviation from the mean temperature field.

[3]By "easterly" we denote the westward zonal wind, and by "westerly"—the eastward zonal wind.

from the WINDII and MLS experiments on UARS and the MFR for the periods of December 1992–March 1993 and November 1993–February 1994, employing temperature observations. The effects of the major SSW during November 2003–March 2004 are examined using SABER temperatures and MFR winds.

The presentation is organized as follows: A brief description of the respective data sets used in the analysis is given in Section 2. These include temperature data from the WINDII and MLS experiments on UARS, the SABER experiment on TIMED, MFR winds and UKMO assimilated temperature and winds data. The results obtained are presented in Sections 3–5 and discussed in Section 6, followed by a summary in Section 7.

2. Observations and data analysis

2.1. WINDII temperature data

The WINDII temperature data are derived from the solar Rayleigh scattering radiances observed at the limb at a wavelength of 553 nm. The retrieval procedure and the data validation have been discussed elsewhere (Shepherd et al., 2001, 2004). The WINDII temperatures from November 1991 to April 1997 provide global coverage from 50°S to 72°N over an altitude range from 70 to 95 km. Orbital constraints and instrument viewing geometry limit the WINDII global coverage between yaw periods from 42° in one hemisphere to 72° in the other and the reverse as a yaw of the satellite takes place approximately every 36 days. As a result, the latitude range 42°S–42°N is viewed all the time independently of the yaw. The WINDII temperatures are retrieved from FOV1 observations, e.g., 45° from the UARS orbit track. The measurements sample horizontal segments of 25 km and are integrated along the line-of-sight direction over a distance of roughly 400 km. On a single day WINDII completes 15 orbits while the Earth rotates beneath it thus providing a full longitudinal coverage over a given latitude circle. Each subsequent day of measurements corresponds to a 20 min change in local time, due to the 57° orbital inclination. Thus about 36 days of observations are required to provide full daytime local time coverage for the latitude range of $\pm 42^\circ$ around the equator.

The daily zonal mean temperatures are obtained by binning the observations on a given day into 10° latitude bins and represent an average of 15 orbits per day. Usually there are three images per orbit within the 10° latitude bin yielding about 45 measurements in a zonal average. Measurements are separated for the ascending or descending WINDII passes because their local times are different. For each latitudinal band there is one data point and one local time for each day of observations corresponding to the average value. Each daily zonal mean value corresponds to the mean local time at which the satellite orbit crossed the 10° latitude bin and thus contains the tidal contribution at that particular local time.

The choice of the period for this study was to some extent dictated by the availability of data, both satellite and ground-based. The most regular WINDII temperature observations were for the period of January 1992–April 1994 and January 1995–April 1997. An earlier study of the seasonal variability of the mesospheric temperatures using WINDII data (Shepherd et al., 2004) established very strong variability at the tropics, which was coupled with variability in the zonal winds and resulted from the effect of the QBO at these latitudes as discussed by Shepherd et al. (2005). The WINDII analysis for the present study employs data from December 1992–March 1993 and November 1993–February 1994. The temperature data are binned in a 10° latitude band from 5–15°N to provide daytime daily zonal mean values in the height range from 70 to 95 km. There are gaps in the WINDII observations between January 31 and February 12, 1993 and January 5–25, 1994.

2.2. MLS temperature data

The MLS temperature data (Wu et al., 2003) analyzed here are derived from the MLS 63 GHz O_2 emissions observations (Barath et al., 1993) on the UARS and cover the height range of 20–90 km. The instrument views 90° to the UARS orbit, which leads to a latitude coverage on a given day from 34° in one hemisphere to 80° in the other. Similar to WINDII, the latitude range of $\pm 34^\circ$ around the equator is near-continuously observed by MLS independently of the yaw. Descriptions of the experimental technique, instrument sampling, the retrieval algorithm and information on precision and validation are provided in Wu et al. (2003). The estimated precision of a single MLS temperature profile from 20 to 90 km height is ~2–15 K with the larger error at higher altitudes. The vertical resolution of the MLS temperature varies from 6 km in

the stratosphere to ~10 km in the upper mesosphere. Comparisons with other data sets suggest a cold bias of 10–15 K above 80 km but this is not expected to significantly affect the temperature variations that are examined here. In the current study, MLS daily zonal means values of the temperature at 5–15°N latitude band are used. These daily zonal means are calculated separately considering the ascending and descending part of the MLS orbit. As in the WINDII case this leads to sampling only one local time on either the ascending or the descending part. While WINDII observes only in daytime, the MLS provide both daytime and nighttime observations within a given latitude band. The MLS temperature data are for the same period of interest as WINDII, namely December 1992–March 1993 and November 1993–February 1994. Strictly speaking, WINDII and MLS do not look at the same volume of air at the same time. However, as we consider daily zonal mean values, the differences are expected to be negligible.

2.3. SABER temperature data

In this study, we have also employed kinetic temperatures measured by the SABER experiment (Mlynczak, 1997; Russell et al., 1999) on board the TIMED satellite. SABER measures daytime and nighttime Earth limb emission vertical profiles in the near to mid-infrared over the range of 1.27–17 μm. The kinetic temperatures in the MLT region are deduced from 15 μm CO_2 emissions and account for the non-LTE conditions in this altitude region (Mertens et al., 2001, 2002). The SABER orbit is nearly sun-synchronous and has an inclination of 73° with respect to the Earth's equator. SABER orbits the Earth in about 90 min providing around 100 temperature profiles during that time. The local time observed by SABER for given latitude in a day is almost the same, and it takes about 60 days to obtain full diurnal cycle coverage. The satellite is yawed every 60 days and over each yaw period SABER alternatively observes a latitude range from 53° in one hemisphere to 83° in the other. The routine temperature retrieval covers the altitude regime from 10 to 105 km with a vertical resolution of ~2 km and resolution along the track of ~400 km. Data may be downloaded from http://saber.larc.nasa.gov. The SABER temperature errors of data version v1.06 are not yet routinely provided. Preliminary estimates give an accuracy of 3 K and a precision of 2 K at the latitude range of 80–100 km (http://www.asd, http://www.larc.nasa.gov/saber/ASDsaber.html). In the analysis that follows, temperature profiles from the ascending and descending part of the TIMED orbit for the latitude range of 5–15°N are used separately to produce daily zonal mean temperature values in the height range from 20 to 100 km. SABER samples only two local times within a day of observations at these latitudes with the local time difference between the ascending and descending parts of the TIMED orbits is 9 h at the most. Therefore, combining all available data within the latitude band would not cancel out the tidal influence on the observations. The daily zonal mean temperature time series comprise the period of November 2003–March 2004 when a major SSW was observed at Northern high and mid-latitudes.

2.4. MFR wind data

Mesospheric wind data obtained from the partial reflection MFR operating at Tirunelveli (8.7°N, 77.8°E) have been utilized in the present study for the periods of December 1992–February 1993, November 1993–February 1994 and November 2003–March 2004.[4] There is a gap of 12 days in the 2003–2004 data set, from January 20 to January 31, 2004, when the MFR facility underwent upgrading. The MFR wind observations cover the altitude range from 70 to 98 km and are daily mean values obtained from 1-h-averaged data accumulated on a daily basis. At altitudes above 80 km, full 24-h coverage of wind measurements is possible, while below 80 km there may be some gaps in the observations during night hours giving a rise of the standard deviation of the data from 0.2 m s^{-1} above 82–84 km to as much as 3 m s^{-1} at the bottom of the MFR altitude range during winter (Rajaram and Gurubaran, 1998). As the data extend over the 24-h diurnal cycle, the daily-mean values above 80 km are practically free of tidal influence.

2.5. UKMO data

We have also used stratospheric fields of daily (at 12:00 UTC, Coordinated Universal Time) zonal mean temperature, and zonal and meridional wind components provided by the UK Meteorological Office (UKMO) from the British Atmospheric Data

[4]For more details on the system and the data set, please see Vincent and Lesicar (1991) and Rajaram and Gurubaran (1998).

Centre (BADC) website at http://badc.nerc.ac.uk. These data have global coverage with 2.5° latitudinal and 3.75° longitudinal steps and are available for 22 pressure levels from 1000 mbar to 0.316 hPa (~0–55 km) with a 1-day temporal resolution (Swinbanks and O'Neill, 1994a; Swinbank and Ortland, 2003). In the current study, we employ zonally averaged data at 1 h Pa (~45 km) over the latitude band of 7.5°N, 10°N, and 12.5°N, centered at 10°N, for the periods of October 1992–April 1993, October 1993–April 1994 and October 2003–April 2004, for consistency with the satellite data used in the current study. The UKMO analyses well represent the major features of atmospheric circulation (Swinbank and O'Neill, 1994b; Orsolini et al., 1997). Systematic errors in the model are reported to be small except near the upper boundary where they are attributed to shortcomings of the parameterizations of gravity-wave drag and radiation.

2.6. Data analysis

To examine the planetary wave variability in the upper mesosphere (70–90 km) during the periods of interest, the data sets were subjected to standard spectral analysis including the Lomb–Scargle periodogram (Scargle, 1982; Hocke, 1998), and Morlet wavelet (Torrence and Compo, 1998). The analysis was carried our separately for the mesosphere and stratosphere with a sampling grid of 1-day resolution, as described below.

The wavelet approach is a favored tool for analyzing time series in which the assumption for stationarity does not hold. The wavelet is simple and closely resembles the modulated planetary wave "packets", which are frequently observed in the MLT variability (e.g. Pancheva and Mukhtarov, 2000). Decomposing the time series into time–frequency space, the wavelet transform is able to determine both the constituent frequencies and how these frequencies vary with time, producing a two-dimensional time–frequency image (e.g. Torrence and Compo, 1998).

In the stratosphere, the analysis of the UKMO assimilated data fields employed a somewhat more complex method of data processing as described by Fedulina et al. (2004). In brief, a Fourier transform based on a least mean squares approach was performed to separate data into large-scale (zonal wave number $m = 0$–2) zonal modes for each latitudinal circle. The time series with daily values of temperature, zonal and meridional winds for the cosine and sine terms[5] for each mode and latitude were constructed. These time series were subjected to Fourier analysis to obtain sets of statistically significant maxima in power spectra. Using a least squares approach and information about the periods existing in the time series, the amplitudes and phases of each harmonics are calculated for two longitudes shifted by a quarter of longitudinal wave length. Then, using the values of amplitudes and phases obtained at these longitudes, each harmonic is separated into westward- and eastward-propagating waves. New time series were generated combining only westward- or eastward-propagating waves with periods less than 20 days. Finally, a wavelet analysis using the Morlet mother wavelet was applied to these time series to investigate variability of the traveling planetary wave activity in the upper stratosphere.

One problem with the wavelet transform is that it requires regularly spaced data points in the time series under consideration, i.e., there should be no gaps in the data. The gaps in the time series considered were filled with a linear interpolation between the neighboring data points. While this prevents the time series from a discontinuity which otherwise could be interpreted by the wavelet as a legitimate periodicity it does not introduce new spectral characteristics to the experimental data set and therefore preserves the original planetary wave spectra.

3. The winter mesosphere/stratosphere at 5–15°N

In February 1993, an SSW event was observed at high and mid-latitudes when the stratospheric temperatures increased by 25 K (e.g. Whiteway and Carswell, 1994; Walterscheid et al., 2000; Hoffman et al., 2002). In the mesosphere the effect of the SSW was expressed as a cooling trend, which at high latitudes reached maximum cooling of—25 K on Days 410–411[6] (February 13–14, 1993) about a week before a warming trend was observed in the high-latitude stratosphere as seen in the NCEP and lidar data. The cooling continued at a slow rate until Day 418 (February 21, 1993), when a

[5]The real and imaginary parts of a wave field, or the behavior of these fields at longitude 0° and 90°W in the case of $m = 1$ and 0° and 45°W in the case of $m = 2$.

[6]Day numbers are counted from January 1, 1992 for the 1992–1993 observations and from January 1, 1993 for the 1993–1994 observations.

warming trend commenced in the mesosphere. The warming in the mesosphere began at the same time as the stratosphere began to cool and recover to its pre-warming state.

The SSW events in February–March 1993 at mid-latitudes at 55°N were examined in detail by Hoffman et al. (2002) (their Table 2). Two warming events, on Day 415 (February 18, 1993) and Day 433 (March 8, 1993) were associated with the reversal of temperature gradient at 30 and 10 hPa pressure levels, enhanced heat flux and the reversal of the zonal mean wind at 1 hPa (~45 km). In the mesosphere, these events were observed 2 days earlier—on Day 413 (February 16) and Day 431 (March 6, 1993).

Four minor SSW events were also observed during the 1993–1994 winter season: on Days 349, 367, 380 and 416 (December 15, 1993, January 2 and January 15, 1994 and February 20, 1994, respectively) (Naujokat et al., 1994; Hoffmann et al., 2002). The effects of these events were observed 2 days earlier in the mesosphere at 55°N. In the mesosphere, the strong minor warming registered on January 3, 1994 was associated with zonal wind reversal from westerlies to easterlies, extending over the entire mesosphere, similar to the minor warming in February 1993 (Hoffmann et al., 2002, their Fig. 4).

The effects of these events on the tropical middle atmosphere are examined as follows.

3.1. November 1992– April 1993

The temperature perturbations observed at the tropics in the winter of 1992–1993 and their relation to the zonal mean winds at middle and low latitudes to a great extent have been discussed by Shepherd et al. (2007). In brief, the period of December 1992–March 1993 was examined in terms of daily mean values of zonally averaged temperatures obtained from the WINDII and MLS experiments at 5–15°N. Ground-based meteor and MFR winds obtained at 54°N and 9°N, respectively, were also considered.

The mesospheric temperature field observed by WINDII and expressed in terms of daily zonal mean temperatures over the latitude range of 5–15°N, centered at 10°N for December 1992–March 1993 is shown in Fig. 1. A temperature cooling of the order of 7 K below the mean value (192 K) can be seen at ~85 km from Day 360 (December 25, 1992) to about Day 385 (January 19, 1993) before descending and forming a second cold anomaly at about 78 km on Day 397 (January 31, 1993). The

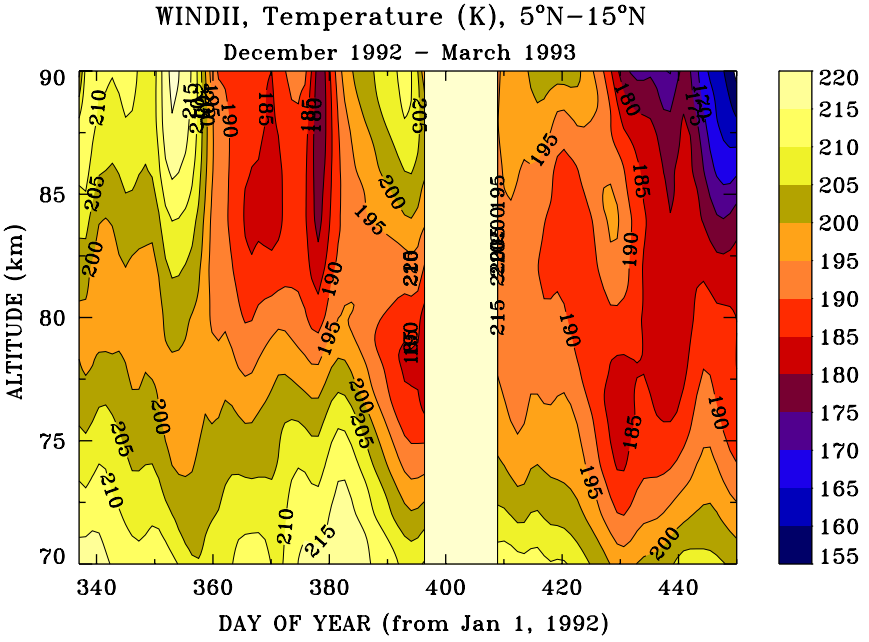

Fig. 1. Height–time cross-section of mesospheric temperatures observed by WINDII over the period from December 1992 to March 1993. The day number is calculated from January 1992.

mesospheric cooling registered around Days 410–411 (February 13, 1993) at mid-latitudes could not be traced directly in the WINDII observations since there was a gap of about 2 weeks in the first half of February 1993. As was already mentioned in Section 2.1 although the height–time cross-section of the mesospheric temperatures in Fig. 1 represents all available WINDII data for the period of interest, the daily mean profiles are for different local times and the data have not been de-trended for tidal influence.

Another SSW event identified by Hoffmann et al. (2002), on March 8, 1993 (Day 433) appears to be well within the period of the cold temperature anomaly seen in Fig. 1, with downward progression of about 1 km d^{-1} and a temperature difference of about 10 K at 78 km. These temperature anomalies extend both vertically and in time into the cold temperature anomaly associated with coupling of the QBO and the semi-annual oscillation at these latitudes and at equinox, as was discussed at length by Shepherd et al. (2005).

The temperature observations from the MLS experiment on UARS for December 1992–March 1993 over the height range from 20 to 90 km were also examined. Height–time cross-sections were produced combining MLS temperature profiles for the same local times on the same days as those from WINDII and the results of this mapping are shown in Fig. 2a and b; thus only the daytime MLS observations are considered in this presentation. Although MLS has much coarser height resolution in the upper mesosphere than WINDII, the main signatures can easily be traced including the large cold anomalies seen already by WINDII between Days 360–380 and Days 420 and 440 (Figs. 1 and 2a, respectively). The MLS cold anomaly around Days 360–380 extends down to 70 km with its temperatures comparable to those observed by WINDII. There is also very good correspondence between the perturbations observed by the two experiments in the Days 420–440 period with cold mesospheric anomalies observed at the time when the SSW at middle and high latitudes (Day 433, March 8, 1993) was observed.

In the stratosphere (Fig. 2b), the stratopause appears at about 50 km height, with three warming periods: Days 360–370 (late December, 1992–early January 1993) and somewhat stronger warming periods around Days 410 and 420–460 (the end of February–March, 1993) consistent with the SSW events observed at 55°N (Hoffman et al., 2002). The enhancement seen at the stratopause is much weaker, only ~10 K in comparison with what has been observed at middle and high latitudes. The correspondence between the warm temperature anomalies in the stratosphere and the cold temperature anomalies in the mesosphere is quite apparent (Fig. 2b). As both data sets have not been de-trended for tidal bias a legitimate question to ask is whether these anomalies do not simply reflect different phases of the diurnal tide. While from general theoretical considerations the diurnal tide is not expected to be strong in the stratosphere, in the mesosphere it can have a considerable influence on the observations depending on season. However, general theoretical considerations and experimental work (Forbes, 1982; Forbes and Wu, 2006) also show that the amplitude of the diurnal tide during winter solstice and at the tropics is not very strong. We will return again to this discussion later in this presentation.

The differences in magnitude of the temperature anomalies registered by WINDII and MLS are not surprising considering the different vertical resolution and data precision between the two experiments as discussed in Section 2. However, the important point is that both data sets reflect cooling above 70 km throughout the mesosphere, which correlates with the warming of the stratosphere over the same period of time.

The MFR daily mean zonal winds at Tirunelveli (8.7°N) in the altitude range from 70 to 98 km shown in Fig. 3 display what would be considered a typical mesospheric winter wind structure with strong westerly winds with wind speeds of as much as 40 m s^{-1}, extending up to 82–85 km before reversing to easterlies, if it was not for the perturbation seen between Days 356 and 390 (December 21, 1992–January 24, 1993). There appears to be a deceleration of the westerly zonal wind extending from 70 to 84 km. A strong wind shear is centered at ~77 km around Day 350 when the wind speed decreases from 40 to −5 m s^{-1} over a period of 2–3 days and stays weak and easterly over a period of 3 weeks (Days 355–375) between 75 and 85 km, before reversing again to its normal winter westerly pattern. Above 84 km, the daily mean zonal wind is easterly throughout the entire period except for the wind reversal around Day 350 and again around Day 380, a westerly signature above the wind deceleration and easterly reversal at around 80 km. Similar to the WINDII temperatures the almost constant vertical shear suggests that these

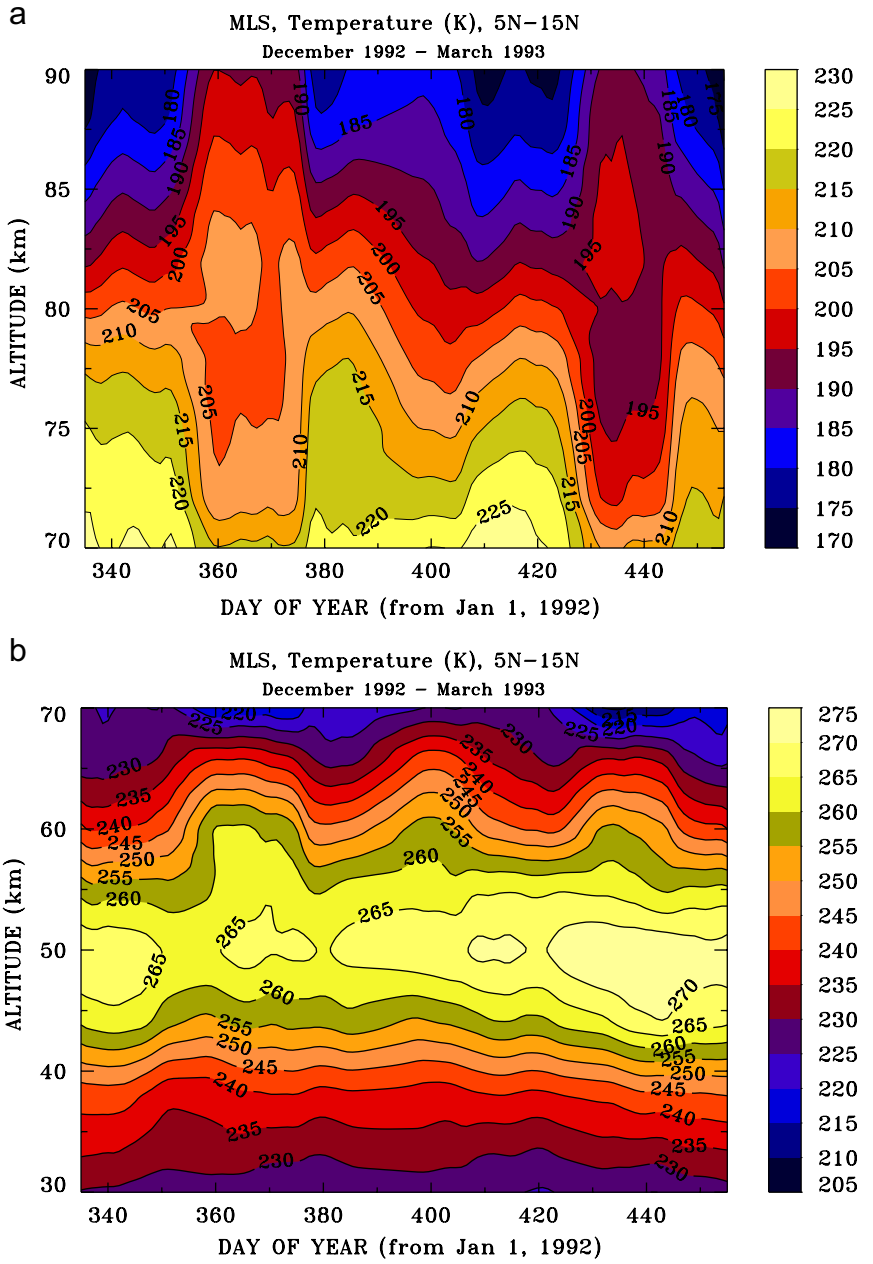

Fig. 2. Daily-mean zonal temperatures from MLS in an altitude-height cross-section at 5–15°N from December 1, 1992 to March 30, 1993—the data sampling as that for WINDII. (a) 70–90 km, height range; (b) 30–70 km height range (see text for details).

changes in the direction of the MFR zonal wind have happened simultaneously at all altitudes, from 70 to 98 km. As the MFR data are averaged over the entire diurnal cycle the wind shear seen here cannot result from tidal effects and changes in the local time as could have been suggested by looking only at the temperature data. There is a downward progression that can be traced both in the easterly winds starting at ~95 km height on Day 335 and ending at 70 km on Day 390 or in the westerly winds—starting at ~90 km height on Days 355–360 and ending on Day 415 at 70 km with a rate of the descent of 0.35 km d^{-1}suggesting an upwelling during the period of Days 355–380. Below 80 km on occasion, there are gaps in the hourly observations from which the daily mean zonal wind values are

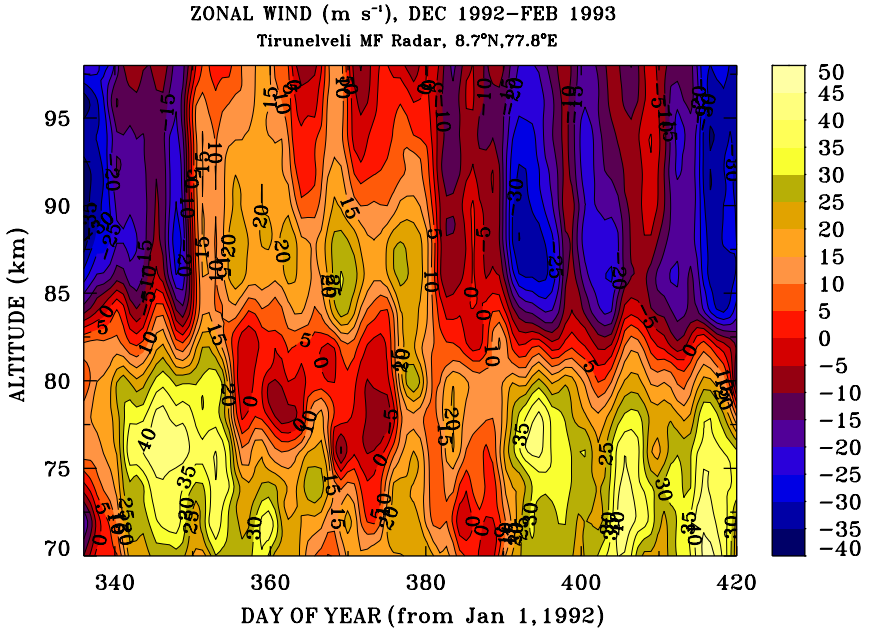

Fig. 3. Height–time cross-section of mesospheric daily mean zonal wind velocity observed at Tirunelveli at 8.7°N over the period from December 1992 to February 1993.

produced and there the data could contain some tidal bias reflected in the slight downward progression of the signatures observed. However, this cannot explain the pattern seen in Fig. 3 above 77–80 km. The vertical wavelength of the perturbation during the period is about 40 km. Some further acceleration of the easterly winds at 87 km is also observed at the end of January 1993 (around Day 397) and February 21 (Day 418). The latter is concurrent with the time of the minor SSW observed at 55°N and the cold temperature anomalies observed by WINDII and MLS.

There is a good correspondence between the cold temperature anomalies around Days 415–440 (February 18–March 15) and the MFR westerly winds observed around Days 397 and 420, which are consistent with the signatures of SSW effects on the mesosphere. The downward propagation of the cold temperature anomaly and, for that matter the easterly zonal wind, suggests an upwelling and adiabatic cooling, consistent with the effects on the mesosphere of the interaction of a transient planetary wave with the stratospheric jet (Liu and Roble, 2002) over the period of Days 360–390 (December 25 1992–January 26 1993).

The descent of 7 km between the two WINDII temperature anomalies, seen in Fig. 1, has a very good correspondence with the easterly zonal wind signature during the same period below 85 km, shown in Fig. 3. However, the wind perturbation appears 5 km lower than the cold temperature anomalies, more in agreement with the MLS temperature observations for the same period (Fig. 2a).

Shepherd et al. (2007) found the cross-correlation between the zonal mean winds at 55°N and 10°N to be 0.52 with a time lag of 15 days for the perturbations observed at the tropics.

3.2. November 1993–February 1994

The WINDII mesospheric daily zonal mean temperatures for the period of November 1993–February 1994 are shown in Fig. 4. Cold temperature anomalies were observed around Day 320 (November 16, 1993), Day 355 (December 21, 1993) and Day 392 (January 27, 1994). The anomaly around Day 320 is possibly associated with the reversal of zonal mean flow during the transition between fall and winter, often observed at mid- and high latitudes (e.g. Shepherd et al., 2004, Fig. 13). The other two anomalies appear about a week after the minor SSW events were observed at 55°N. Unfortunately, there are no WINDII data at these latitudes for the period between Days 370 and 390, so it is impossible to follow the temporal development of this anomaly.

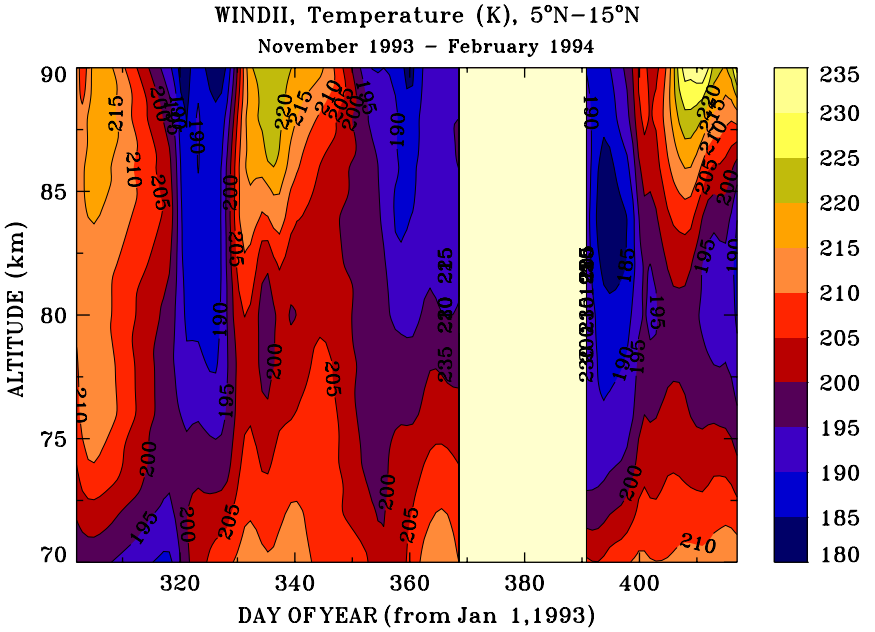

Fig. 4. Height–time cross-section of mesospheric daily zonal mean temperature at the latitude range of 5–15°N from WINDII (left panel) over the period from November 1993 to February 1994. The day number is calculated from January 1993.

There is a good correspondence between the cold temperature anomalies seen in the WINDII data and those observed by MLS, in spite of the difference in height resolution and data precision. The cold temperature anomaly seen around Day 395 and 83 km can also be traced in the temperature data from the MLS experiment, both in the mesosphere and stratosphere, Fig. 5a and b. As before, for consistency of the comparison with the WINDII observations, the MLS profiles given in Fig. 5a are daily zonal mean values at the same local times as WINDII. The daytime MLS cold anomaly begins around Day 385 and lasts until about Day 405 descending to about 75 km. It is followed by a warming around Day 410 similar to WINDII although lacking the level of detail seen in the WINDII data. The cooling in the mesospheric temperatures around Day 395 appears at the beginning of the stratospheric warm anomaly shown in Fig. 5b, which lasts until Day 440 (spring Equinox, March 20, 1994); it peaks around Day 416 (February 20, 1994) at the same time as the minor SSW was observed at 55°N. This is also true for the temperature enhancement following December solstice, Days 360–370. This also concerns the other cold temperature anomalies seen in November 1993 and mid-December.

The height–time cross-section of the MFR daily mean zonal wind, shown in Fig. 6, indicates some planetary wave activity with the westerly phase descending over time with the rate of 4 km/day. The westerly zonal winds are not very strong, of the order of 10–15 m s^{-1} and in general are weaker than those observed during the same period in 1993. Some increase in the westerly winds may be seen at ~85–90 km around Days 325, 355 and possibly 395, which might correspond to the cold temperature anomalies seen in the daily zonal mean temperature data, but no definite parallels can be drawn. Except for the easterly anomaly at Days 304–320 (first half of November) at 75–85 km, the zonal wind is predominantly westerly and possibly reverses to easterlies above about 90 km.

Examining the mesospheric temperature and MFR zonal wind fields, it is not surprising that in this particular case the cold temperature anomalies seen in the satellite data both by WINDII and MLS do not correspond directly to the easterly phase of the zonal mean wind, in the way it was seen in the January 1993 observations. Other reports also indicate that the zonal wind and temperature perturbations during the winter of 1993–1994 were weaker than those observed during the 1992–1993 winter season (Rajaram and Gurubaran, 1998; Manney et al., 1994) possibly related to the phase of the QBO cycle at these latitudes (e.g. Shepherd et al., 2005; Sridharan et al., 2003). In addition, while the satellite data are zonally averaged, the

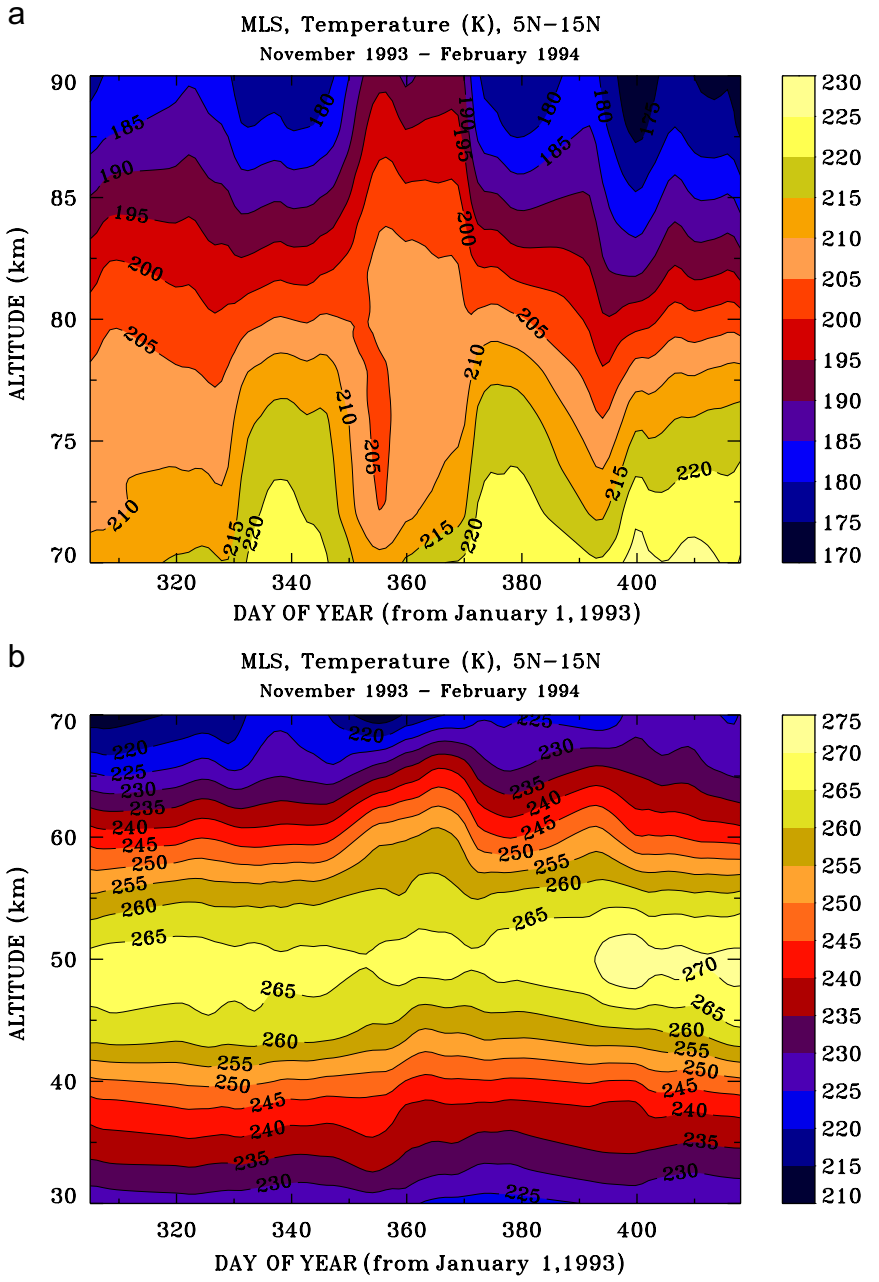

Fig. 5. Same as in Fig. 2, but for November 1993–February 1994.

MFR winds are only at a single location along the latitude range used in the comparison. Thus local perturbations do not necessarily agree with the zonal mean over this latitude range.

3.3. November 2003– March 2004

The effect of SSW on the low-altitude mesosphere was further examined employing temperature data from the SABER experiment on the TIMED satellite for the period of Days 305–440 (November 1, 2003–March 15, 2004). A major warming was registered at high latitudes in the stratosphere, beginning in early January 2004 which led to nearly 2 months of vortex disruption with high-latitude easterlies in the middle to lower stratosphere (Manney et al., 2005). The temperatures at 2 hPa were lower than usual in both January and

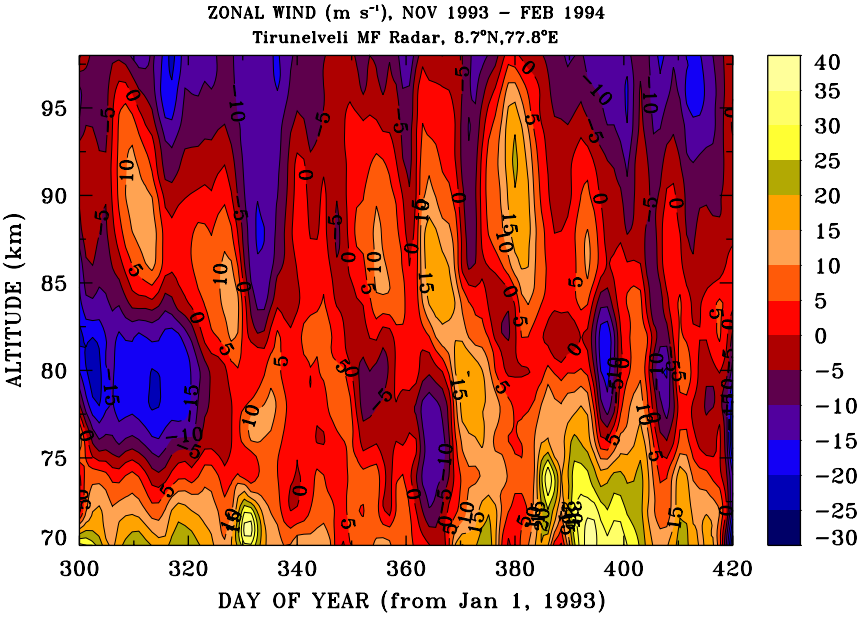

Fig. 6. Height–time cross-section of daily mean zonal wind velocity observed at Tirunelveli at 8.7°N over the period from November 1993 to February 1994.

February 2004 while February was the coldest in the 26-year record, over three standard deviations below the average).[7]

At mid-latitudes, the beginning of December 2003 was marked by a minor SSW in the middle and upper stratosphere over Central and Eastern Asia (60°E–160°E), when the temperature increased by 25–30 K with a peak of 240 K at 120°E–160°E (Gordienko et al., 2007, Fig. 6). Another area of high temperatures (240 K) over Europe and Western Asia developed into a major warming in the beginning of January, after which the middle stratosphere returned to normal winter conditions. At the end of January, a new warming pulse developed at the middle stratospheric levels. The disturbed temperature pattern continued for almost 4 weeks. A final warming is observed at the beginning of March 2004.

In the tropical mesosphere (70–90 km height), the temperature field as seen by SABER exhibits significant variability with height and over time as can be seen in Fig. 7a and b marked by cold anomalies (~175 K) around Days 320–340 (November 15–December 5, 2003), seen in 7b, for the descending data set. The cold anomaly deepens with height above 80 km and extends throughout Days 305–380 (December 1, 2003–January 15, 2004. The variability range in the ascending data is larger for the descending sub-data set as can be seen in Fig. 7a. There is a deep cold anomaly in early November, ~Day 315, extending down to at least 60 km, which is likely a result of the fall/winter transition of the mesosphere and the reversal of the zonal mean flow. However, with the exception of the small temperature inversions around Days 327 and 341 the cold December anomaly seen in the descending data, Days 340–360 is also seen here but is ~10 K higher in magnitude. Both ascending and descending cross-sections show warm temperature anomalies around Days 360–370 and another around Day 375 (December 25, 2003–January 4–9, 2004) extending portion of the orbit to about 80 km. At higher altitude, these warm anomalies are replaced by cold ones. If it were not for the temperature inversions seen around Days 326 and 341 in the ascending and those around Days 400–410 in the descending data set the two data sets show very similar patterns of warming of the mesosphere at the end of December and early January, followed by mesospheric cooling which reaches down to ~70 km and lasts till the end of the period considered, March 15, 2004, with temperatures of ~175 K. As in the earlier data and also the results reported by Mukherjee et al. (1987), we see a pattern of cooling and warming of the mesosphere before the cold temperature anomaly corresponding to the SSW sets in.

[7](http://www.cpc.ncep.noaa.gov/products/stratosphere/winter_bulletins).

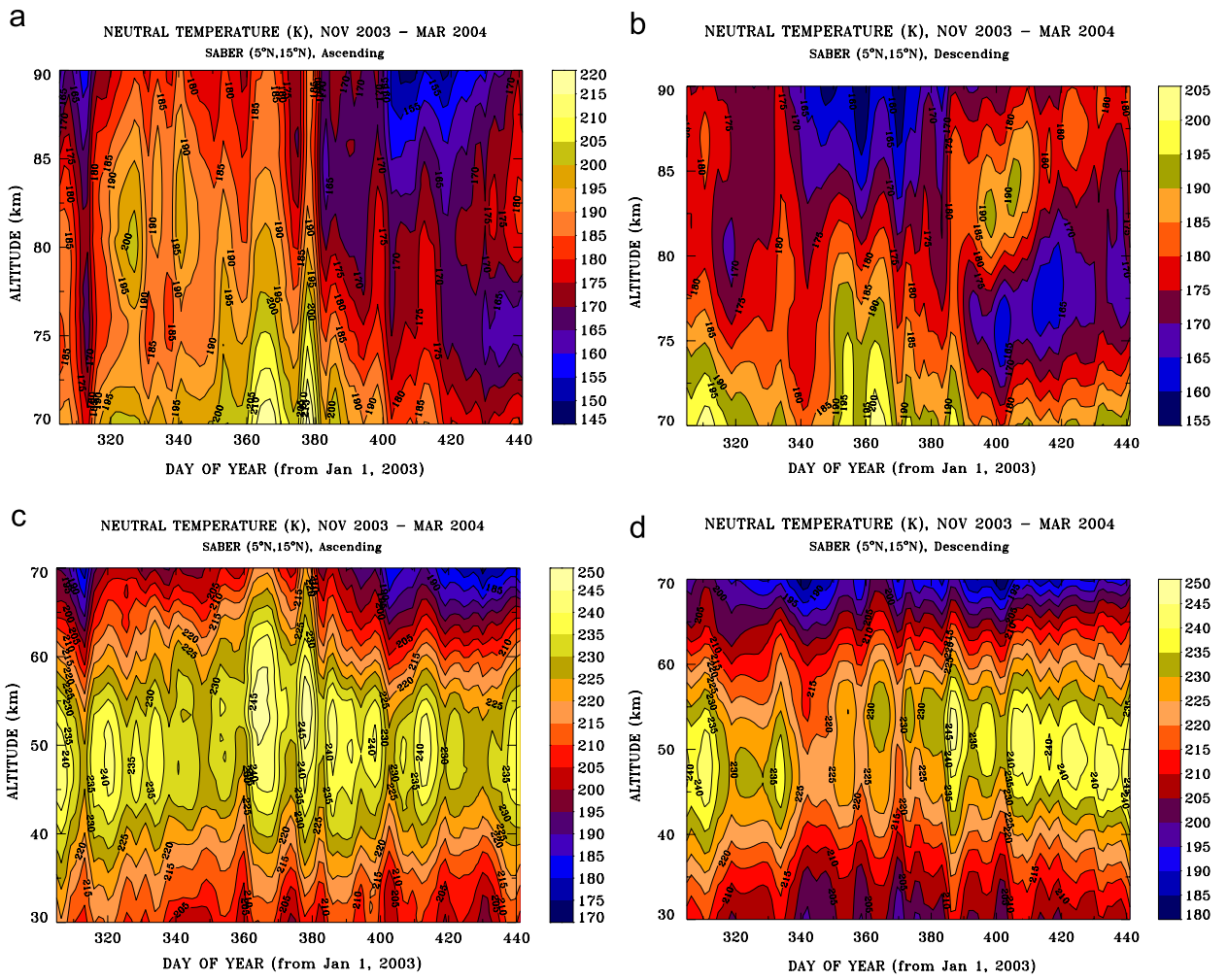

Fig. 7. Daily-mean zonal temperatures from SABER in an altitude-height cross-section at 5–15°N from November 1, 2003 to March 30, 2004. (a) at altitudes from 70 to 90 km, ascending part of the orbit; (b) at altitudes from 70 to 90 km, descending part of the orbit; (c) at altitudes from 30 to 70 km, ascending part of the orbit; (d) at altitudes from 30 to 70 km, descending part of the orbit. The day number is calculated from January 2003.

In the stratosphere, the warm anomaly around Days 360–370 has a maximum of 245 K and its effect extends well into the mesosphere and toward the lower stratosphere as can be seen in Fig. 7c. Another warm anomaly of 245 K around Day 411 (February 15, 2004) is seen in both ascending and descending data and in Fig. 7c and d and corresponds to the cold anomaly seen at the same time in the mesosphere. A comparison between the peak stratopause temperatures observed by MLS in 1992–1993 and 1993–1994, and by SABER in 2003–2004 also shows that the 2003–2004 winter stratopause was about 30 K colder.

The time of these temperature anomalies correlates well with the SSW registered at middle and high latitudes, from which the one at the beginning of January 2004 is a major event. Thus what was seen as a possible connection during the SSW events from the early 1990s observed in the WINDII and MLS data, here becomes most apparent through the SABER observations. There also seems to be a more rapid response of the tropical middle atmosphere to the SW events observed at mid-latitudes in comparison with the response seen in the 1992–1993 observation, for example—possibly related to the strength of the SSW perturbation.

According to the MFR wind observations at Tirunelveli, the daily mean zonal wind at 84–98 km, shown in Fig. 8, reversed from a relatively weak easterly in November 2003 to westerly in early

December 2003 when a minor SSW was observed at these longitudes at middle and high latitudes. The westerly zonal wind peaks around mid-December reaching a maximum of 25–30 m s^{-1} and decelerated before reversing again to easterly winds at the end of December–early January 2004 when the major SSW event was observed at middle and high latitudes as shown by the NCEP and UKMO assimilated data (e.g. Gordienko et al., 2007) and also seen in SABER temperatures. There is a gap in the MFR observations from January 19 until the end of January 2004 but in spite of that the daily mean zonal wind remains easterly until mid-March 2004. The easterly winds were not strong, 0–20 m s^{-1} except for the period around Day 440, when they reached the rate of 43 m s^{-1} at 86–88 km height. This is also the time of the last SSW event (Gordienko et al., 2007). There is a very good correlation between the cold mesospheric anomalies observed by SABER during this period, the warm stratospheric temperature anomalies and the easterlies enhancements as can be seen in Figs. 7 and 8.

4. Planetary wave activity in the mesospheric temperature and wind fields

4.1. December 1992– April 1993

The Morlet wavelet of the WINDII temperatures at 86 km over the period of December 1992–March 1993 revealed the presence of a 4- and 7-day wave in early December and a 16-day wave present throughout the entire month peaking around December solstice, Day 355. Toward mid-January an 8-day wave is also detected. All these have amplitudes of ~4 K. Another 4-day wave is observed in mid-February and a 14–16-day wave is also detected in March 1993 (Fig. 9a). Because of the gaps in the WINDII data in the 5–15°N latitude band, no wave structures were observed between Days 380 and 405, as well as no short-period waves have been identified.

With the MLS data arranged in the same local times as WINDII, there is a very good correspondence between the planetary wave signatures seen in the MLS temperature wavelet at 86 km (Fig. 9c) and those revealed in the WINDII data (Fig. 9a). This similarity can be traced in the signatures from Days 335–380 (December 1992–early January 1993) with a 14-day wave extending through the period and accompanied by 8-day and weaker 4-day waves around Days 370–380 (early January). The remaining period of interest is dominated by a 16-day wave with a peak around Day 420 (February 23, 1993), similar to WINDII. The amplitude of the waves identified in the MLS data is about a factor of 2 smaller than those seen in the WINDII data.

In the stratosphere at 50 km (Fig. 9e), the planetary wave activity remains similar although much weaker to that seen in the mesosphere by the

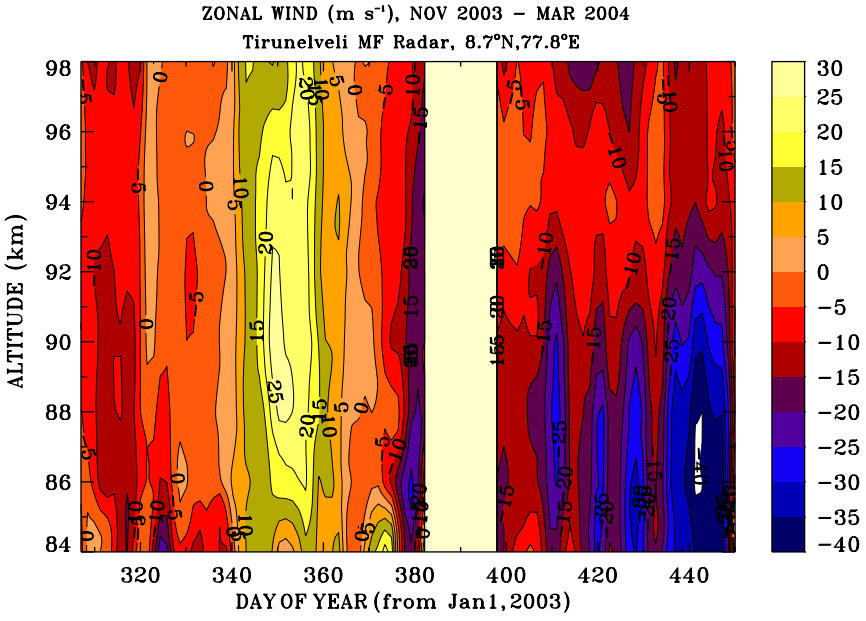

Fig. 8. The daily mean zonal wind at Tirunelveli, (8.7°N, 77.8°E) for November 2003 till March 2004.

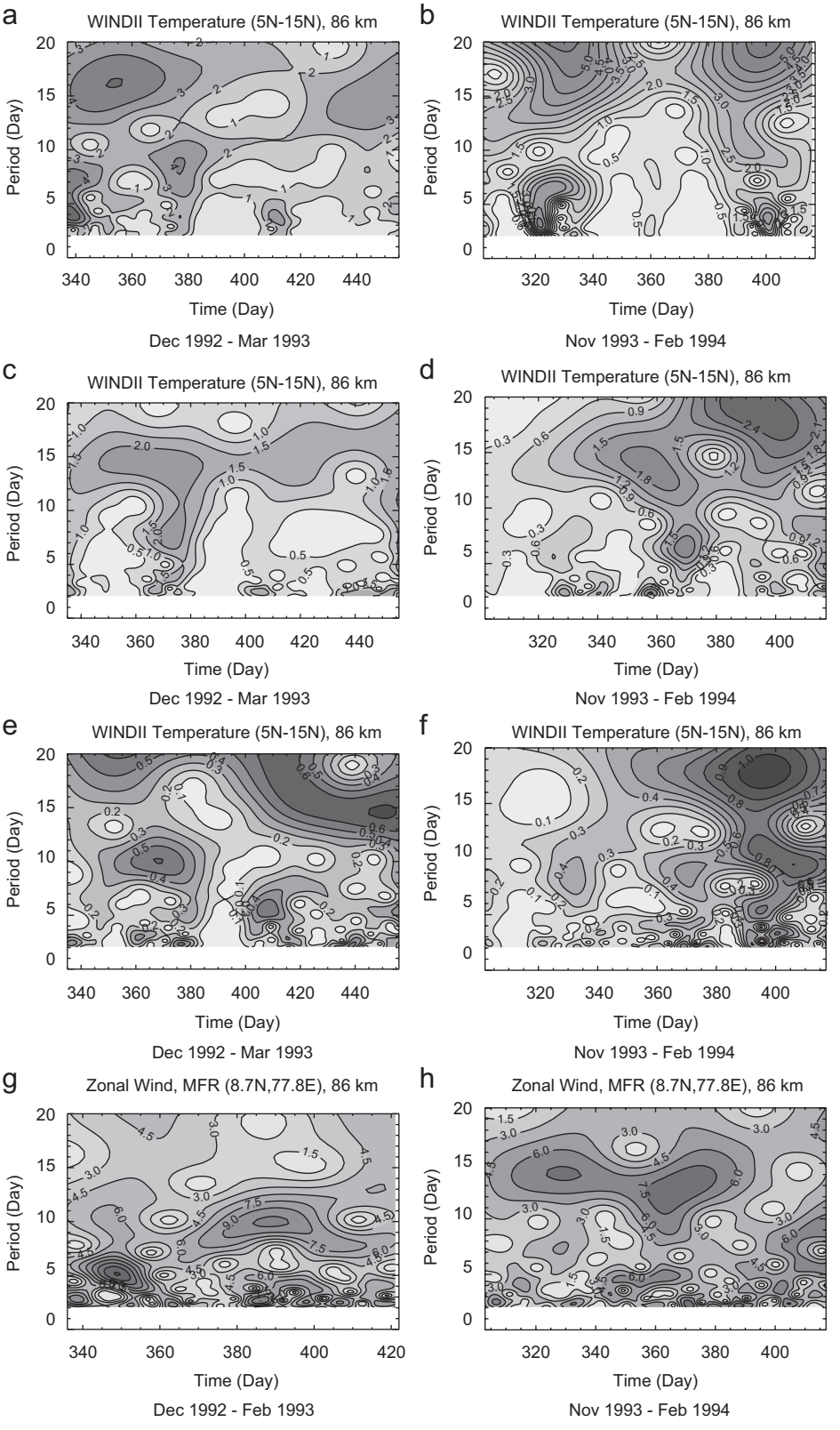

Fig. 9. Morlet wavelet for December 1992–April 1993 (left column) and November 1993–February 1994 (right column) for: (a,b) WINDII zonal mean temperature at 86 km; (c,d) MLS zonal mean temperatures at 86 km, sampling as for WINDII; (e,f) MLS zonal mean temperatures at 50 km, sampling as for WINDII, and (g,h) MFR zonal wind observations at 86 km height.

two instruments. Four-day and 11-day waves can be seen on Days 360–390 (the end of December 1992–early January 1993); a 4–5-day wave around Day 410 and a 14–16-day wave around Days 420–430 (February 23–March 6, 1993) are also observed. These similarities indicate the coupling of the two regions (stratosphere and mesosphere).

With respect to the MFR zonal wind data at 86 km, the observed planetary wave signatures are stronger but their periods are mostly between 2 s and 12 days as can be seen in Fig. 9g. A 5-day wave with an amplitude of 14 m s^{-1} dominated the period before December solstice (~Day 350) and is also accompanied by a 9–11-day wave with amplitudes ~6 m s^{-1} (Fig. 9f). The period between Days 370 and 410 is dominated by a strong 10-day wave and amplitude of 11 m s^{-1}, centered at around Day 385 (January 19, 1993), accompanied also by a 2-day wave with amplitude of 9 m s^{-1}. However, no correspondence between these planetary wave signatures and those seen in the temperature data can be seen.

At the time of the minor SSW around February 18, 1992 and the warming in early March, 1993 (Days 412–433), a 16-day wave can be seen both in the WINDII and MLS temperature wavelets at 86 and 50 km. Some long-period waves also appear to be present in the MFR zonal wind wavelet around Days 410–420, but its development cannot be followed further for lack of observations.

4.2. December 1993– February 1994

The correlation between the WINDII and MLS observations and planetary wave activity reflected in these observations can also be seen over the period of November 1993–February 1994 given in Fig. 9b,d and f. The WINDII temperatures at 86 km from November 1993–February 1994 revealed a strong 3-day wave in mid-November 1993 (Day 320), with amplitude of 5 K coupled with a 7-day wave. The November and the late-January–February interval appears more dynamically active with signatures of 7- and 15–20-day periods around Day 325 and 4–5, 10 and possibly 18-day around Days 385–415. Their amplitudes are comparable of the order of 5 K (Fig. 9b). No planetary wave activity is observed between Days 345 and 390, partly resulting from the lack of observations as was shown in Fig. 4.

On a first glance, the MLS temperature wavelet at 86 km (Fig. 9d) differs from that seen by WINDII, mostly in the range between Days 340 and 380, when WINDII does not show significant planetary wave activity—only signatures of 3- and 8-day periods and amplitudes of the order of 1 K can be seen. However, the signatures observed by MLS during the entire periods are weaker than WINDII which makes the 3–4 day wave seen around Day 360 only slightly stronger. The 14-day wave and amplitude of 2 K around Day 355 appears in the WINDII data as well, but coupled with other longer-period waves, which are not observed by MLS. Finally there is a good agreement between WINDII and MLS toward the end of the period, February 1994 when long-period waves of ~18 days are observed. In the stratosphere, at 50 km (Fig. 9f) the planetary wave activity is very weak but still showing 6-, 11- and 18-day signatures at the end of January 1994, Days 390–400, which still can be traced in the mesosphere both in WINDII and MLS.

The wavelet of the daily mean zonal wind observed at Tirunelveli at 86 km in 1993–1994 shown in Fig. 9h shows 7- and 14-day wave around Day 330, similar to what is seen in the temperatures and a strong 13-day wave around Days 360–370 similar to that seen by MLS but with a different phase.

It appears that there is a delay of about 2 weeks in the peak of the planetary waves seen at 10°N and the minor SSW reported by Hoffmann et al. (2002). The dominant planetary wave signatures observed in the time interval of Days 350–420 (December 15, 1993–February 15, 1994) are a 7-, 16- and 18-day waves.

4.3. November 2003– March 2004

The Morlet wavelets for the ascending and descending parts of the SABER orbits at 86 and 50 km are shown in Fig. 10a–d. In the mesosphere, a strong 7-day wave is observed around Days 370–380, both in the ascending and descending data sets, following the temperature enhancements seen in the stratosphere at the beginning of January 2004. This wave appears together with 9–12 day waves, which extend to the end of January–early February, 2004 (~Day 400). There are series of 2–3 day wave outbursts throughout the period and at both altitudes, which might result from the sampling of the data rather than being a real planetary wave. This is particularly apparent in the temperature wavelets at 50 km (Fig. 10c and d), as there are

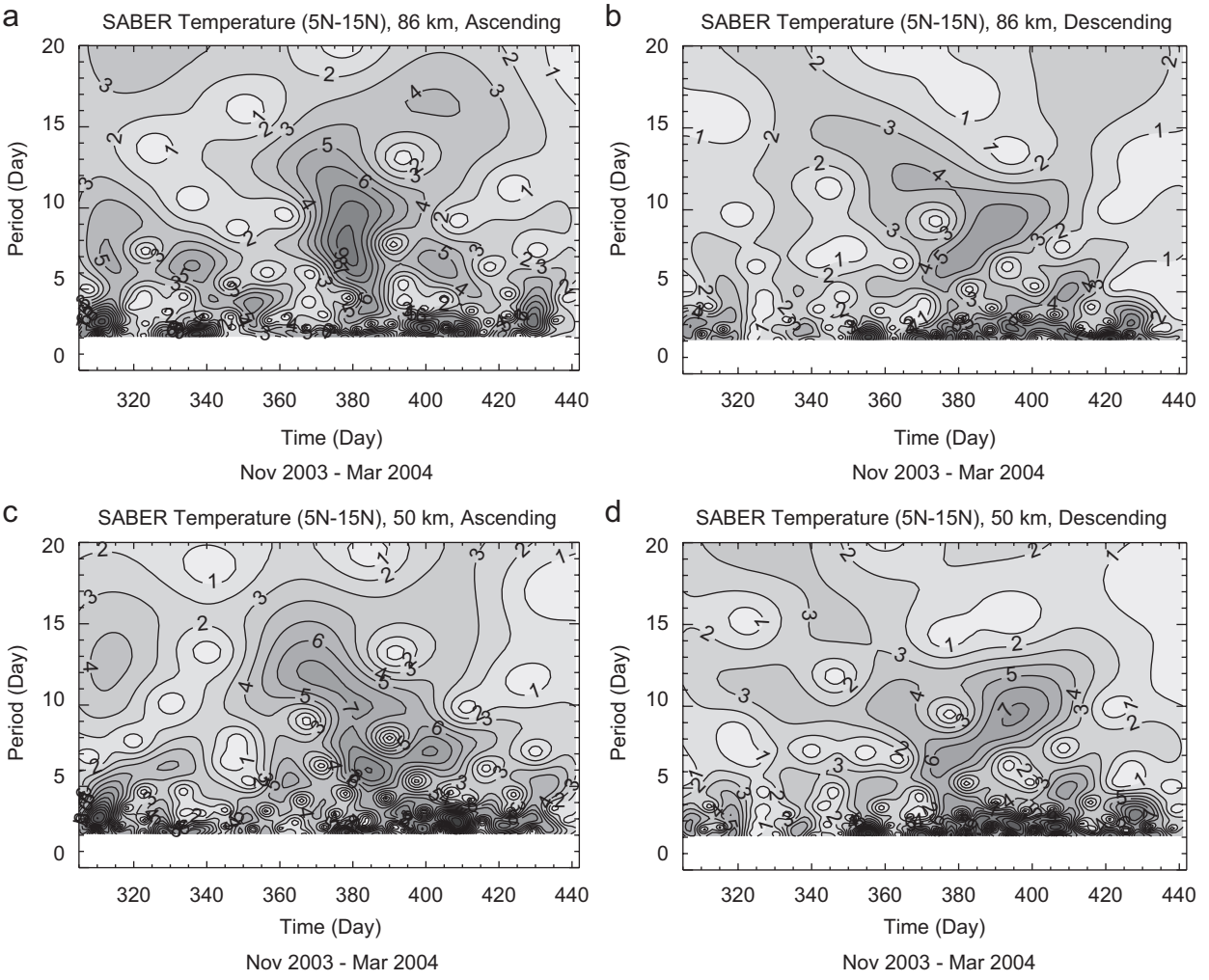

Fig. 10. Morlet wavelet for the SABER zonal mean temperatures from November 2003 to March 2004 for the ascending part of the orbit (left panel) and the descending part of the orbit (right panel) at 86 km (a,b) and 50 km (c,d).

no observational evidence that 2-day wave exists in the stratosphere. It is interesting that the amplitude of the waves observed at 86 and 50 km are practically identical. To examine the origin of these waves and their possible relation to the SSW events, we turn now to the spectral analysis of the UKMO stratospheric assimilated data.

5. Planetary wave activity in UKMO stratospheric assimilated fields

Wavelet spectral analysis has also been applied to the UKMO stratospheric assimilated fields of temperature, zonal and meridional winds at 1hPa pressure level (~50 km height) to examine the large-scale planetary wave activity at the tropics during the period of October–April of 1992–1993, 1993–1994 and 2003–2004. The data are examined for the presence of stationary, traveling planetary waves, westward- and eastward-propagating with wave numbers $m = 1$ and 2. As in the satellite data analysis, only planetary waves with periods of 2–20 days are considered. A summary of the quasi-stationary planetary waves and traveling planetary waves identified at 1 hPa pressure level is given in Tables 1 and 2, respectively.

The temperature wavelet for the period of October 1992–April 1993 for westward-propagating waves with wave numbers $m = 1$ and 2, respectively, are shown in Fig. 11a and b. Here we are concerned

with the period corresponding to the available WINDII, MLS and MFR data, namely December 1992–March 1993. The amplitudes of temperature planetary waves at 1 hPa are quite weak, and well below 1 K. The zonal mean temperatures indicate a westward-propagating $m = 1$ wave with a period of ~7.5-day and an amplitude of 0.5 K around December solstice 1992, possibly coupled with 12-day wave (Fig. 11a). This is similar to the 7–12-day signature centered at around Day 370 in the MLS wavelet at 50 km (Fig. 9e) although no 14–16-day waves are observed at the end of February, seen in

Table 1
Quasi-stationary planetary waves at 1 hPa

Season	Zonal wave number	Parameter	Amplitude	Phase (deg)	Time interval
Dec 1992–Mar 1993	$m = 1$	T	1 K	240	End November–early December
			0.9 K	330	Mid-February
			0.9 K	270	Mid-March
		Zonal wind	14 m s^{-1}	290	Mid-November
			12 m s^{-1}	150	Early December
			6 m s^{-1}	180	End January
			4.5 m s^{-1}	180	Early March
	$m = 2$	T	1 K	130	December solstice
			1 K	110	End January
			0.6 K	140	~10 February
			0.4 K	65	End February–early March
			0.7 K	160	March equinox
		Zonal wind	7 m s^{-1}	160	Early December
			2 m s^{-1}	110	End January
			2 m s^{-1}	10	Mid February
			2.5 m s^{-1}	120	Early March
Nov 1993–Feb 1994	$m = 1$	T	2.1 K	300	First half December
			1 K	295	First half January
			1.5 K	330	March equinox
		Zonal wind	21 m s^{-1}	190	November–early December
			7 m s^{-1}	60	End January
			12 m s^{-1}	150	March equinox
	$m = 2$	T	1 K	125	Mid-November
			1.4 K	120	Mid-December
			0.5 K	120	First half February
			0.6 K	140	Early March
		Zonal wind	7 m s^{-1}	140	End November
			7 m s^{-1}	120	Mid December
			5 m s^{-1}	100	10 January
			3 m s^{-1}	145	Mid-February
			5 m s^{-1}	90	Mid-March
Nov 2003–Mar 2004	$m = 1$	T	5 K	90	Mid-December
			2 K	355	January
			2 K	80	End January/February
			1.9 K	80	Mid-March
		Zonal wind	30 m s^{-1}	230	End November–early December
			6 m s^{-1}	20	First half January
			20 m s^{-1}	150	End February
	$m = 2$	T	2.5 K	10	December
			1.9 K	165	January
			1 K	20	Second half February
		Zonal wind	7 m s^{-1}	20	Early December
			10 m s^{-1}	80	End December
			16 m s^{-1}	150	Second half January
			5 m s^{-1}	10	Early February
			7 m s^{-1}	65	Mid-March

Table 2
Traveling planetary waves at 1 hPa

Season	Zonal wave number	Parameter	Westward wave	Time interval	Eastward wave	Time interval
Dec 1992–Mar 1993	$m = 1$	T	7.5d, 12d	December	5–10d	Dec–Feb
		Zonal wind	14d, 6–7d	Dec–Jan	14d	November
		Meridional wind	14d, 3–4d	January	10d, 5–16d	January–February
	$m = 2$	T	3d	Late January	3d	Jan–Feb
			3–5d	Late February	12d	Dec–Jan
			10–12d	February–March		
		Zonal wind	9d	December	6d	December
			5d, 9–10d	January		
			18d	February–March		
		Meridional wind	12–16d	Mid January	2d	Late January
			12–16d, 5d	Mid February		
Nov 1993–Feb 1994	$m = 1$	T	9d	Mid December	14d	Early December
			16–18d	January	7.5d	January
			10d	February	4d	February
		Zonal wind	8d, 12d	Late December	14d	December
			10d	Late Feb–Mar		
		Meridional wind	10d	January/late February	5d	Early January early February
			4d	December	8d, 14–16d	November
	$m = 2$	T	6d, 10d	Late Dec	9–17d	Nov–Dec
			14d	Late Jan	5d	Jan, Feb
			7d	February		
		Zonal wind	5d	Dec–Jan, Feb	9–16d	November
			12d	Late December		
		Meridional wind	6d	Dec–Jan	6d	November
			14d	Late December		
Nov 2003–Mar 2004	$m = 1$	T	7d	December	7d	November
			14d	Nov–Dec	16–18d	December
			10d	Feb–Mar	10d	February
		Zonal wind	12–18d	Nov–Dec	16d	November
			7d	Late December	7d	January
			9d	February	8–12d	February
		Meridional wind	8d	Late December	8d	December
			8d	Late February	10d	February
					14d–16d	November
	$m = 2$	T	8d, 10–12d	Late December	14d (12–16d)	Late Dec
			6d	February, March		
		Zonal wind	7d	Late December	7–12d	Nov–Dec
					18d	February–March
		Meridional wind	8d	Late December	8–10d	Nov–Dec
			6d	February, March	9d	February–March

the satellite data. The westward-propagating $m = 2$ wave is also weak with a 3d signature and an amplitude of 0.5 K, centered at the last decade of January 1993 (Fig. 11b). A very weak 9–12-day signature is also observed through February and March 1993. The eastward-propagating $m = 1$ and 2 waves (not shown here) are also very weak.

The planetary wave activity in the temperature field during the period of November 1993–February1994 for wave numbers $m = 1$ and 2 is illustrated by Fig. 11c and d. The period was marked by the presence of westward-propagating $m = 1$ waves with periods of 9–10 days at the end of December 1993 and early January, 1994 and the second half of February, 1994, as well as a 16-day wave centered at mid-January 1994. A westward $m = 2$ planetary wave with a period of 10 days was also observed at the end of December and appeared coupled with a

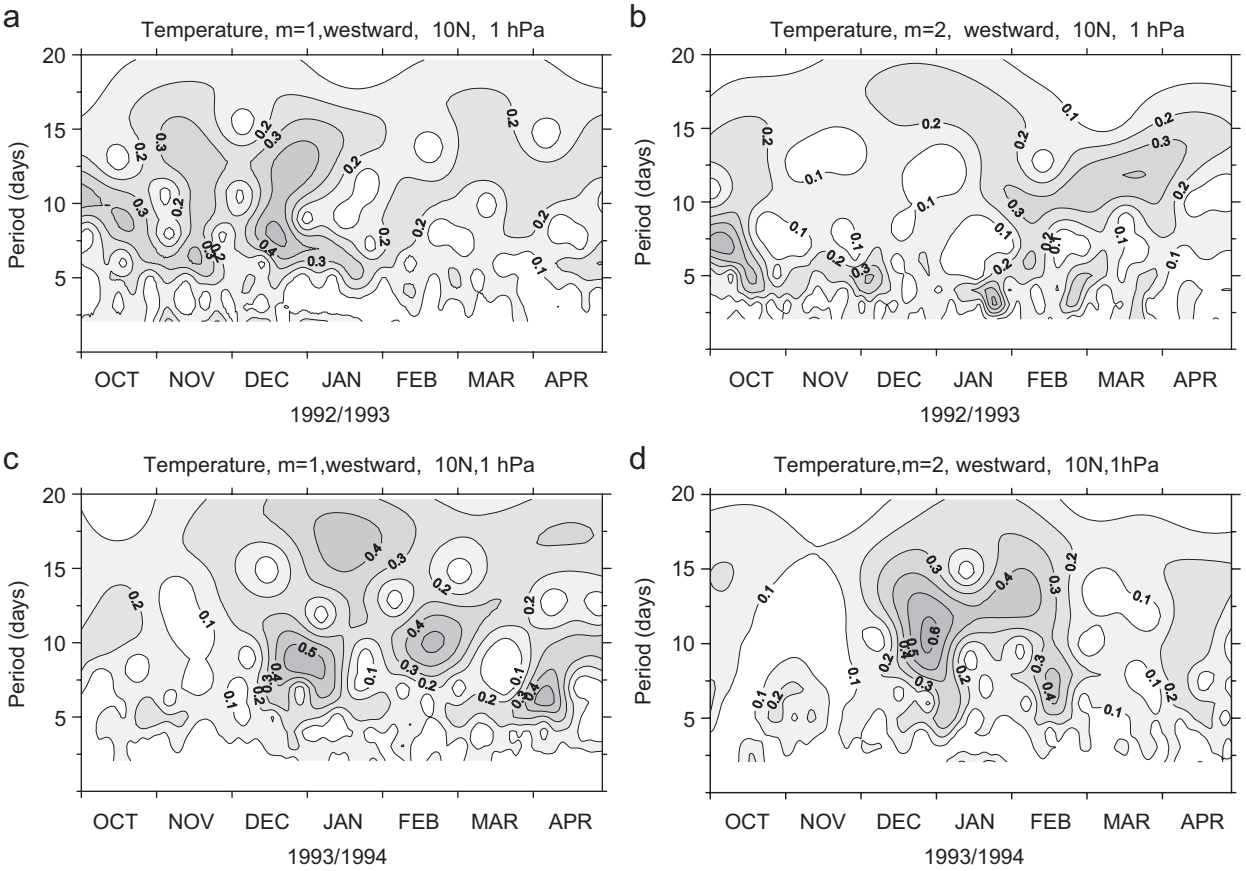

Fig. 11. Westward traveling planetary waves with wave number $m = 1$ (left column) and $m = 2$ (right column) in the zonally averaged UKMO assimilated data at 1 hPa for temperature: (a,b) 1992–1993, and (c,d) and 1993–1994.

7–12 day wave at the end of January–early February, 1994 (Fig. 11d).

The wavelet of the zonally averaged zonal wind field at the 1hPa pressure level during October 1992–April 1993 is shown in Fig. 12a and b. A westward-propagating $m = 1$ wave with a period of 14 days and an amplitude of $6.5\,\mathrm{m\,s^{-1}}$ appears in mid-January, 1993 and is the dominant feature from December 1992 to March 1993. Another perturbation with a period of 6–7-day and amplitude of $\sim 3.5\,\mathrm{m\,s^{-1}}$ is present following December solstice 1992 until the end of January 1993. The eastward $m = 1$ planetary waves are weak with an amplitude of less than $1\,\mathrm{m\,s^{-1}}$ through the entire period.

Weak 8-day and 12–13-day westward $m = 1$ waves with an amplitude of $6\,\mathrm{m\,s^{-1}}$ were observed in the zonally averaged zonal wind field at the end of December 1993, while a strong 10-day wave with an amplitude of $9\,\mathrm{m\,s^{-1}}$ dominated the period between late February and early March, 1994 (Fig. 12c and d). The end of December 1993 and early January 1994 are also perturbed by a strong 5-day westward wave with $m = 2$ and amplitude of $13\,\mathrm{m\,s^{-1}}$, as can be seen in Fig. 12d.

The UKMO assimilated temperature, zonal and meridional winds at 1 hPa pressure level for the time interval of October 2003–April 2004 were also used to analyze the large-scale planetary wave activity during that period and the results are presented in Fig. 13, for $m = 1$ and Fig. 14, for $m = 2$. As can be seen the period from mid-December 2003 to early January 2004 is marked by a strong westward-propagating planetary wave activity in all three fields (Fig. 13a,c and e). The dominant wave $m = 1$ has a period of 7–8 days. Other perturbations with a period of about 14-day are also seen in late November and early December 2003, while a 10-day $m = 1$ wave is also seen at the end of February, 2004. There is a very strong correlation between the planetary waves seen in the temperature field and those in the zonal and meridional winds; however, their amplitudes are weak, only of a few degree

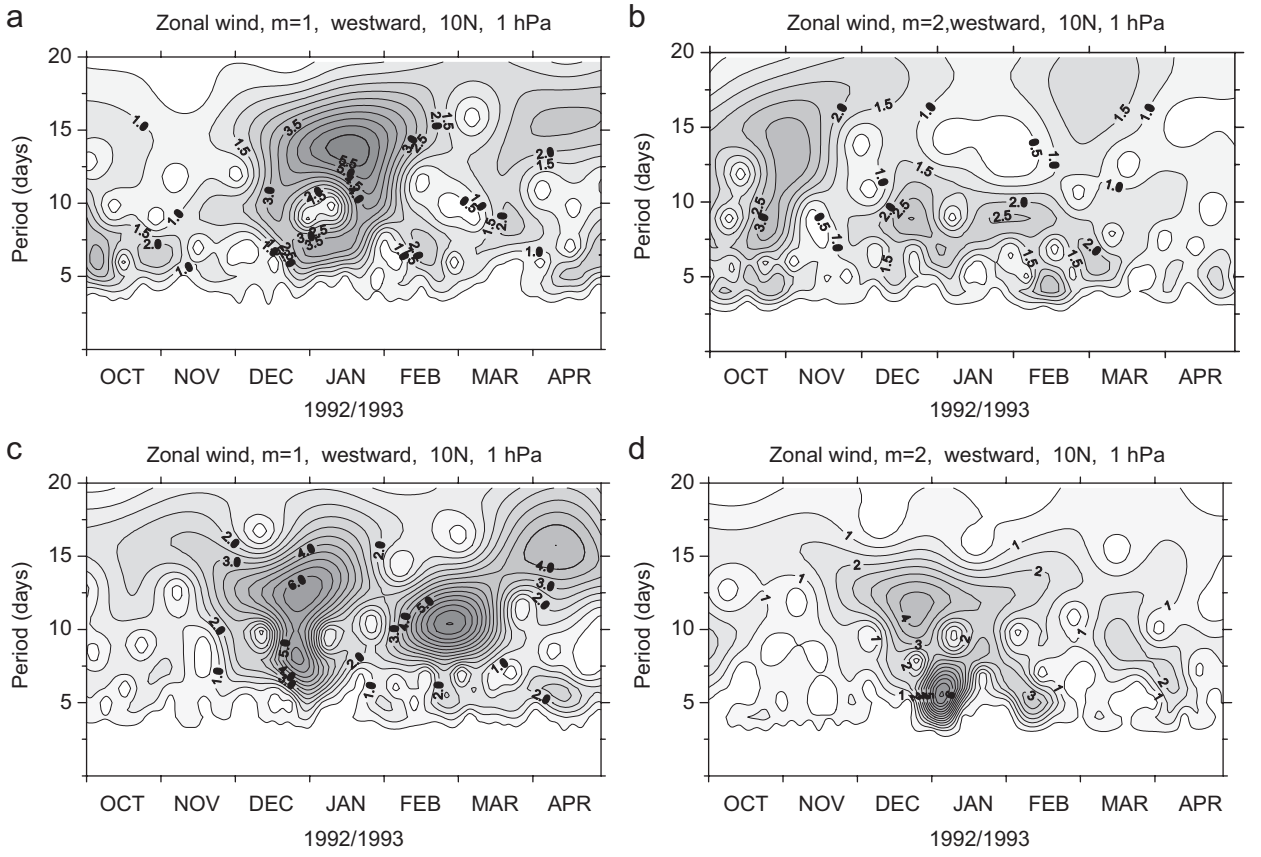

Fig. 12. Westward traveling planetary waves with wave number $m = 1$ (left column) and $m = 2$ (right column) in the zonally averaged UKMO assimilated data at 1 hPa for zonal wind: (a,b) 1992–1993, and (c,d) 1993–1994.

Kelvin and $\mathrm{m\,s^{-1}}$, respectively. The eastward-propagating $m = 1$ waves are comparable in magnitude with their westward counterpart and generally indicate waves, peaking at the same times and periods as the westward-propagating signatures. This is most apparent in the eastward $m = 1$ zonal and meridional winds shown in Fig. 13d and f, respectively.

A similar pattern is observed also in the $m = 2$ wavelets for the westward- and eastward-propagating signatures as shown in Fig. 14. A very strong wave with a period of 7–8 days is observed at the end of December 2003 dominating the planetary activity in the three fields, as can be seen in Fig. 14, left column. Other 6–8 day signature can also be seen at the end of February and mid-March 2004 (these are the times of the SSW events). In comparison with the eastward $m = 1$ and 2 waves during the winters of 1992–1993 and 1993–1994, the eastward $m = 2$ waves in November 2003–March 2004 are very prominent. This is not surprising considering the strength of the SSW observed. For the temperature, the most dominant signature is a 14-day wave at the end of December, at the same time when the $m = 1$ waves peak. However, the zonal and meridional wind fields are dominated by a 7–11-day wave at the end of November, 2003. Another 18-day and 10-day waves are present at the end of February–early March 2004 in the zonal and meridional winds, respectively (Fig. 14, right column).

Finally, to put in context the planetary wave variability and its possible relation to the SSW events and to aid the discussion on this relationship examples of the stationary planetary waves with $m = 1$ and 2 for the 2003–2004 winter season are given in Fig. 15.

6. Discussion

The dynamics of the winter mesosphere (November–February) is marked by considerable gravity wave

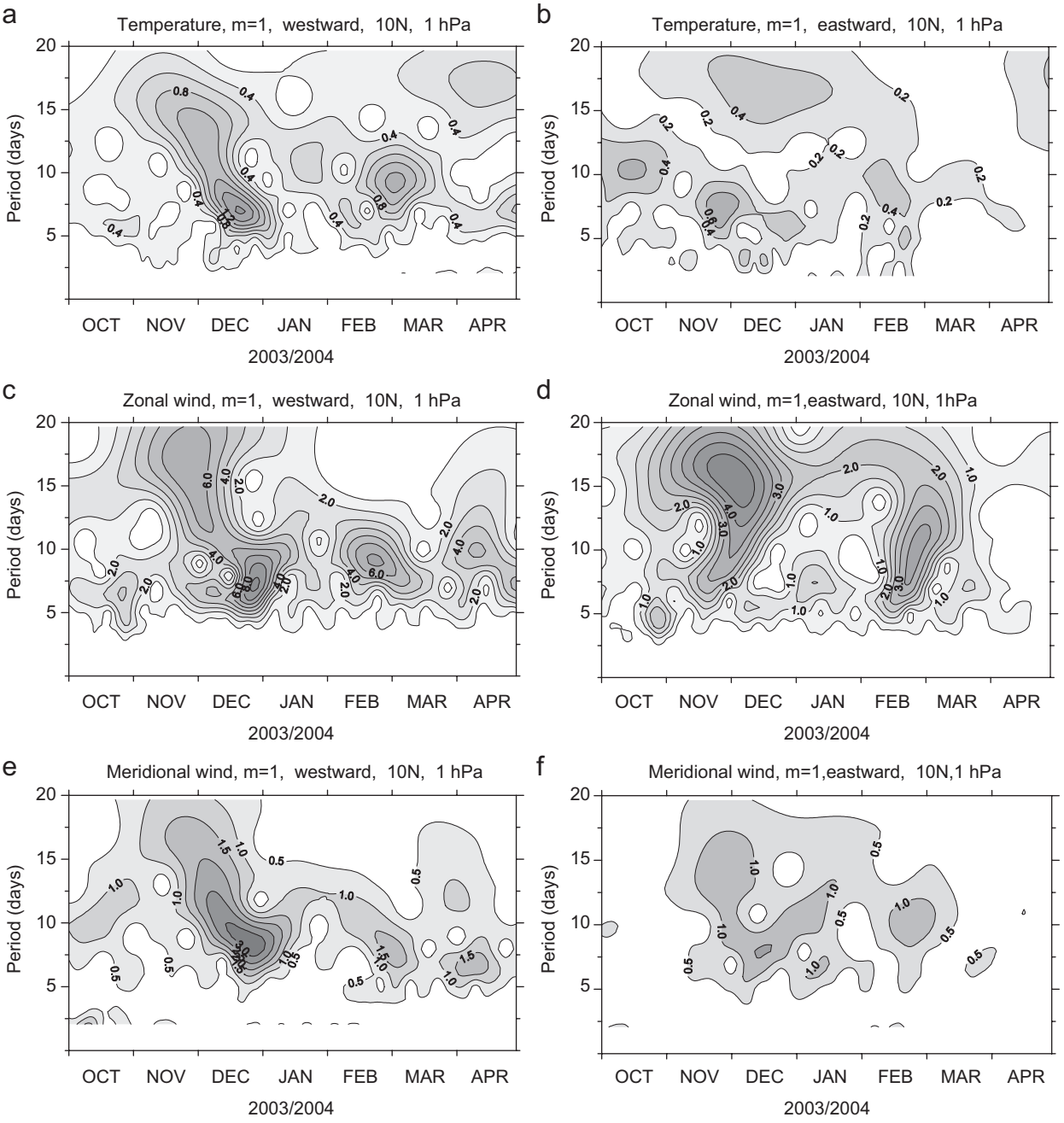

Fig. 13. Traveling planetary waves, westward (left column) and eastward (right column) with wave number $m = 1$ for 2003–2004 in the zonally averaged UKMO assimilated data for: (a,b) temperature field; (c,d) zonal wind field, and (e,f) meridional wind field.

activity and events of SSW, which in turn are coupled with planetary wave activity in the mesosphere and appear as cold temperature anomalies. As was first described by Matsuno (1971) and further elaborated on and demonstrated by Liu and Roble (2002), the key mechanism for the generation of SSW is the growth of upward-propagating planetary waves from the troposphere and the interaction between the transient wave and the mean flow. Matsuno's (1971) model also showed that there is a mesospheric cooling accompanying the SSW, which was also experimentally observed. The interaction decelerates and/or reverses the westerly winter stratospheric jet and induces a downward circulation in the stratosphere and upward circulation

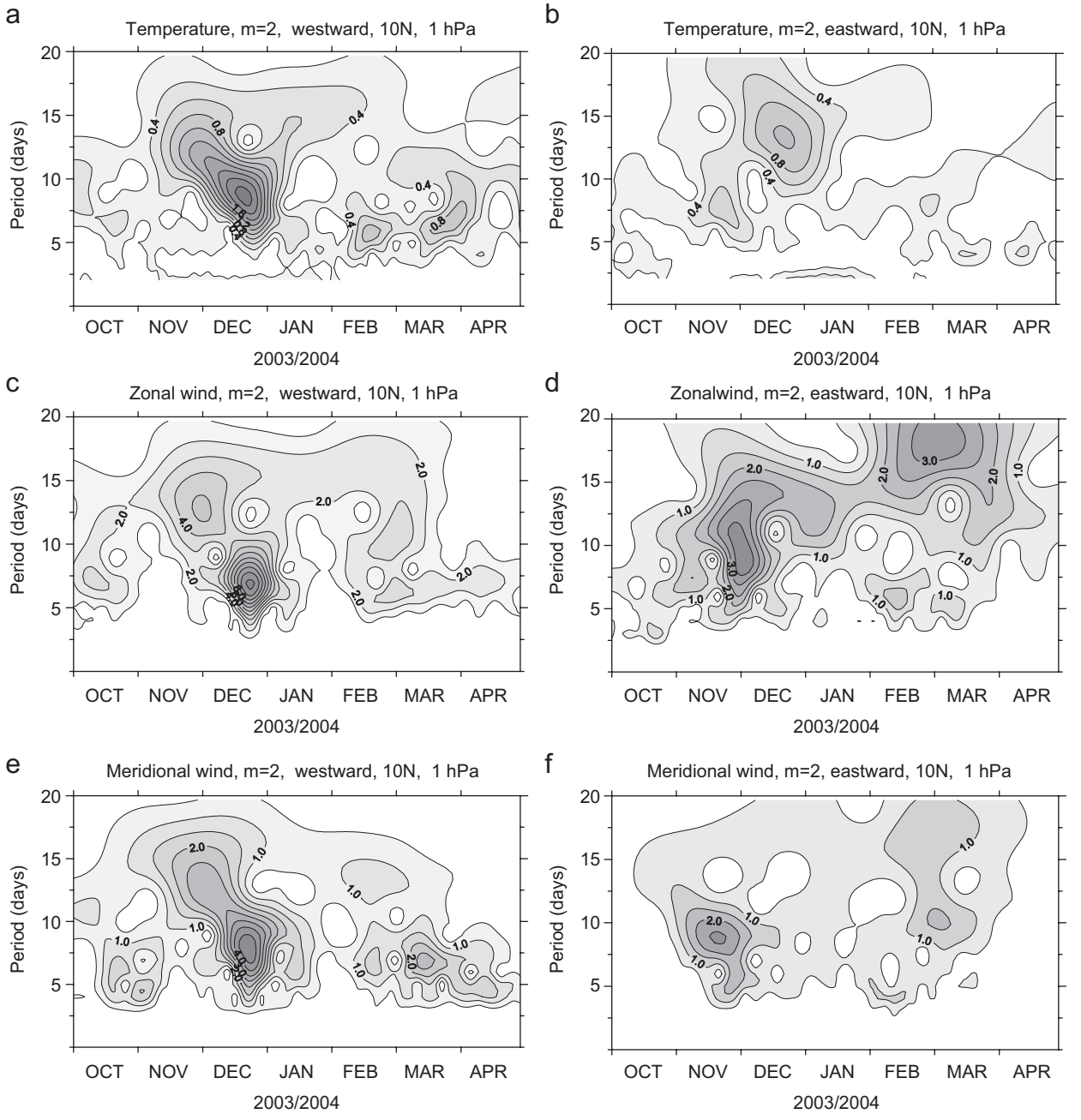

Fig. 14. Traveling planetary waves, westward (left column) and eastward (right column) with wave number $m = 2$ for 2003–2004 in the zonally averaged UKMO assimilated data for: (a,b) temperature field; (c,d) zonal wind field and (e,f) meridional wind field.

in the mesosphere, which in turn leads to adiabatic warming/cooling in the stratosphere/mesosphere, respectively. The main mechanism for planetary wave amplification is considered to be the resonant wave (wave 1 and wave 2) amplification under winter conditions (Liu and Roble, 2002, and the references therein). As was shown so far, there is a cooling of the tropical mesosphere at the time of the SSW, similar to what has been observed at middle and high latitudes and generally consistent with Matsuno's model.

One shortcoming of the satellite mesospheric temperature data is that they are biased by the presence of migrating tides depending on the local times at which the daily zonal mean temperatures are

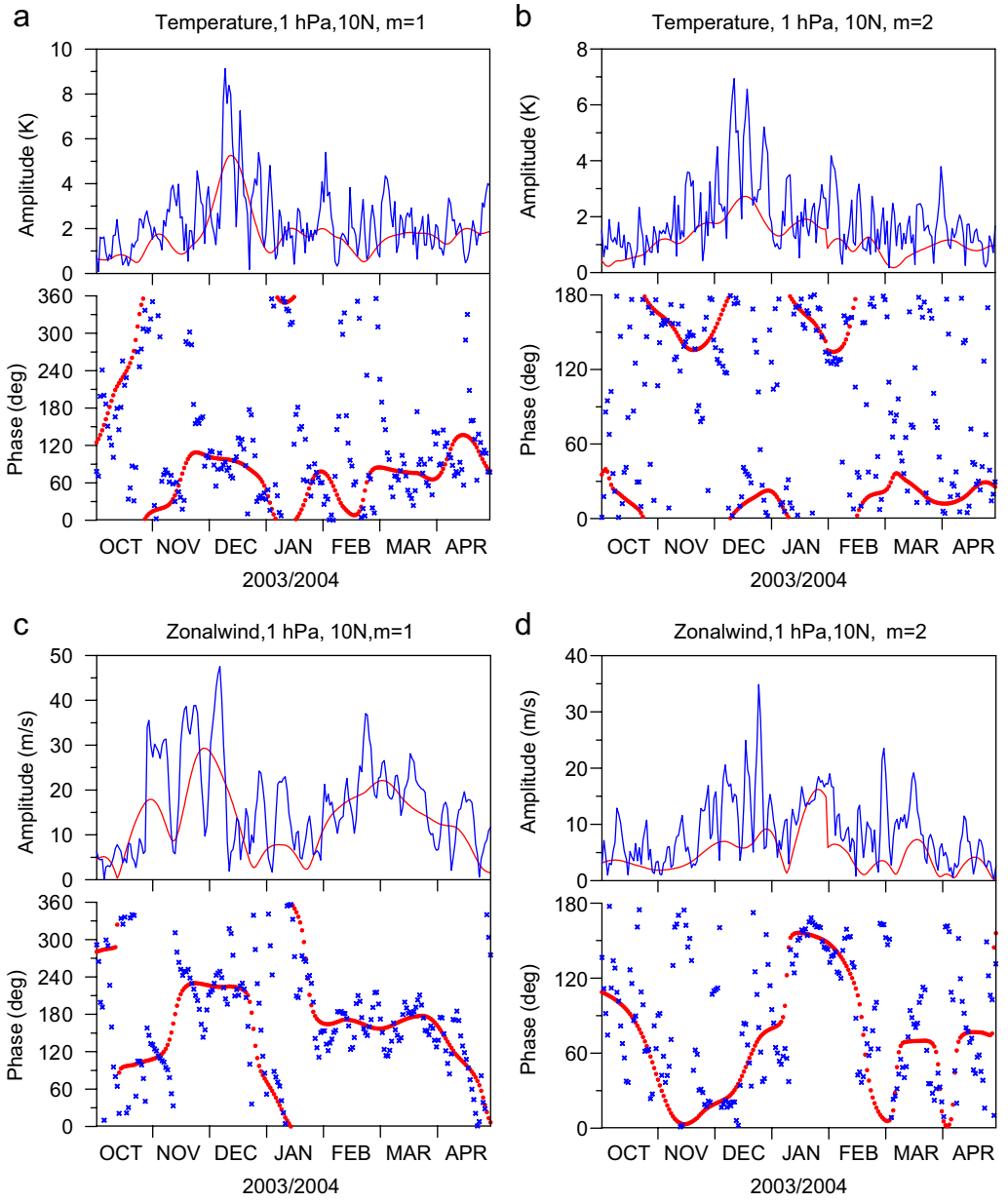

Fig. 15. Amplitude and phase of the planetary waves (blue) and stationary planetary waves (red) at 1 hPa for the period from October 2003 to April 2004 in the zonally averaged UKMO assimilated data for: (a,b) zonal wave number $m = 1$ for temperature and zonal wind fields (left column) and (c,d) zonal wave number $m = 2$.

obtained. In the WINDII case determining the diurnal tide, contribution cannot be done since these are only daytime observations. In the MLS and SABER cases, such determination requires different format of the data processing as it will take about 36 and 60 days, respectively, to obtain full 24-h local-time coverage. In this it is helpful to consider the results of Forbes and Wu (2006) on the retrieval of tidal parameters from the MLS temperature observations. According to that study, the diurnal tidal amplitude and phase in January at 10°N and 86 km height are of the order of 4.5 K and −8 h, while for the semi-diurnal tide they are 2.4 K and 1.5 h, respectively. However, as we consider only planetary waves with period greater than 2 days, this tidal bias should not affect the results from the wavelet analysis.

It is well accepted now that stationary and traveling waves with the same zonal wave number when present together would interfere and this interference will result in transient fluctuations of the wave amplitude with time (Smith, 1985, and references therein). Smith (1985) has shown that when traveling and stationary waves interfere in the lower stratosphere they will do so throughout the upper stratosphere and the lower mesosphere and the amplitude will grow simultaneously at all altitudes as the waves come into phase with each other. As Salby (1981) has shown, the amplitude, phase and frequency of the free wave, including the 16-day wave, all depend on the background wind and therefore would not be expected to remain constant during an SSW. The relationship between the stationary wave and the traveling wave $m = 1$ is best illustrated by the results obtained from the analysis of November 2003–March 2004 data shown in Fig. 12, Figs. 13, 14 and 10. However, the results presented suggest that at the 5–15°N latitude band the interaction between the stationary wave and the westward traveling waves at the time of the SSW events leads to an enhancement more of the 7-day wave $m = 1$ rather than longer period waves like the 16-day wave, although signatures with 12–20 day periods are also observed. All these signatures are consistent with the effect of SSW on the tropical mesosphere and in particular on the mesospheric temperature field.

Quasi-stationary planetary-scale waves (SPW) are dominant features of the winter hemisphere. The first report on the presence of SPW at the tropical mesosphere was by Venne et al. (1988) employing temperature observations from the pressure modulator radiometer. Smith (1996, 1997) and Wang et al. (2000) examined the global distribution of stationary planetary waves in the zonal and meridional winds fields observed by the high-resolution Doppler interferometer (HRDI) and WINDII on UARS and showed that the SPW are present throughout the winter mesosphere. Wang et al. (2000) showed that the amplitude of zonal wind SPW zonal wave number $m = 1$ and 2 at 90 km height, which is the closest in height to the mesospheric temperature observations and 10°N does not exceed 5 and 3 m s^{-1}, respectively during the period of December/January 1992–1993 and 1993–1994. The SPW $m = 1$ was weaker throughout the entire meridional/height cross-section and no conclusions could be made for the SPW at 90 km and at the tropics.

The wavelet analysis applied to the data considered revealed the presence of a variety of planetary-scale perturbations from which westward-propagating waves with periods of 5-, 7-, 10- and 14–16 days are most frequently observed. As the modeling works of Salby (1981) and Forbes et al. (1995) have shown, these periods are associated with the atmospheric manifestation of the first three Rossby normal modes of zonal wave number 1 ((1,2), (1,3) and (1,4) or 5-, 10- and 16-day waves, respectively) in winter. As Salby (1981) has shown, the westward-propagating 16-day wave is expected to manifest itself within a large band of periods from 12 to 20 days, as a result of the interaction of the traveling planetary waves with the background zonal mean flow or stationary planetary waves (e.g. Smith, 1985; Forbes et al., 1995).

In the stratosphere during the three winter seasons considered, westward-propagating signatures at 1 hPa with $m = 1$ and period of 14 days (or 12–16 days) were often observed in December–January in all three assimilated data fields (temperature, zonal and meridional winds) as was shown in Figs. 11–14 and summarized in Tables 1 and 2. This is likely to be a signature of the 15-day westward-propagating $m = 1$ wave which prevails in the Northern hemisphere winter with a maximum in December–January (e.g. Fedulina et al., 2004 and references therein). During the periods of December 1992–March 1993 and November 1993–February 1994 westward-propagating waves with $m = 1$ and 2 and periods of 4–6-day are also observed in December, January and February in agreement with the results of Fedulina et al. (2004), who after analyzing 10 years (1992–2001) of the UKMO assimilated 1 hPa data have shown that this signature is associated with the first symmetric normal mode of the 5-day wave which is know to have a life time of 20–40 days. The 5-day wave has a minimum at 10°N during solstices, which can account for the small amplitudes determined by the wavelet analysis.

According to Garcia et al. (2005) in the winter of 2003–2004, the planetary waves in the stratosphere were eastward propagating with wave numbers $m = 1$ and 2, a period of 7.1–14.4 days, and amplitude of 1 K (1.2 and 1 K, respectively). In the MLT region only waves with periods of 3–3.8 days were detected. Planetary waves with wave number $m = 2$ and period of 1.7–1.9 days and amplitude of 3 K were also present in the PW spectrum from SABER, for the periods considered by Garcia et al.

(2005). All these waves were identified as Kelvin waves. In general, there is a good correspondence between the planetary wave signatures identified in our analysis and those reported by Garcia et al. (2005).

In the upper mesosphere, the wave associated with the horizontal structure of the (1,1) mode is found to occur at periods between 6 and 7 days, although is commonly known as a "5-day wave". In the satellite temperatures at 86 km no 5-day wave was observed over the two winter seasons of 1992–1993 and 1993–1994, while a 4–6-day perturbation centered on Day 350 (preceding December solstice) appears as the dominant feature in the MFR zonal wind with an amplitude of $15\,m\,s^{-1}$. This is consistent with the results of Wu et al. (1994) and Talaat et al. (2001) showing that the 5-day (1,1) wave in the upper mesosphere wind field does not display large amplitudes near the solstice periods. Their analysis using observations from the HRDI experiment on UARS at 95 km showed a 5-day wave in November 1992 and 1993 at 10°N with amplitude of $\sim 15\,m\,s^{-1}$.

The periods of Days 320–350 and 390–440 show signatures of mesospheric temperature inversions in the SABER observations between 77 and 85 km for the ascending and 80–90 km for the descending data sets, shown in Fig. 7a and b. These temperature inversions most likely result from the diurnal tide bias since as was mentioned earlier both data sets contain profiles with local time covering the entire diurnal cycle and thus will be affected by the tidal phase and that particular local time as have been described in detail by Meriwether et al. (1998) and Meriwether and Gerrard (2004). However, not all local times are sampled during the ascending or descending part depending on the orbit position along the globe. This can potentially lead to oversampling of given local time and thus tidal phase in comparison with other local times. The observed temperature inversions can also result from the dynamical interaction of gravity waves with the mean flow as experimental (e.g. Leblanc and Hauchecorne, 1997) and model (e.g. Hauchecorne and Maillard, 1990) results have shown. On the other hand, recent model results (Sassi et al., 2002) have shown that the magnitude of the inversions highly correlates with the amplitude of vertically propagating planetary waves, while gravity waves play an essential indirect role by setting up a critical line in the upper mesosphere where Rossby waves beak in the mesospheric surf zone. Therefore in the wavelet analysis, waves with periods of less than 48 h are deliberately not considered.

The MFR wind wavelet for the season of 1993–1994 indicate strong 12–16 day wave throughout the month of January 1994 with an amplitude of $7.5\,m\,s^{-1}$ (Fig. 9(g) which seems to result from the short reversals of the background zonal mean flow above ~80 km from westward to eastward, shown in Fig. 6. These results are consistent with the results by Luo et al. (2002). These authors show a peak in the 16-day wave amplitude of $7\,m\,s^{-1}$ at 86–87 km in early January 1994 and again at the end of February and early March 1994 (their Fig. 5) at equatorial latitudes (Christmas Island, 2°N).

7. Summary

Results have been presented on the possible effects of SSW events on the tropical mesosphere for the period of December 1992–March 1993, November 1993–February 1994 and November 2003–March 2004 at 5–15°N. Five data sets for these periods, from WINDII, MLS, SABER, MFR and the UKMO were analyzed to examine the daily mean temperature, zonal and meridional winds structure in the mesosphere and their relationship to perturbations observed in the stratosphere. All three satellite data sets contain some tidal bias due to their orbit configurations and sampling. This tidal bias is expected to be more significant in the upper mesosphere where the tidal amplitude maximizes. In order to make the results more consistent the MLS data were arranged according to the same date and local time as WINDII. The results obtained are in very good agreement in spite of the differences in the vertical resolution of the two data sets. All three satellite data sets showed the presence of cold temperature anomalies at the time of temperature increase in the tropical stratosphere, correlative in time with the SSW observed at middle and high latitudes. This cooling of the mesosphere was preceded by short cold- and warm-temperature anomalies in the mesosphere, while no significant changes were observed in the stratosphere. The presence of tidal bias in the mesospheric data could in general lead to some degree of warming and cooling depending on the tidal phase at the local time of the respective observations, but from what we now know about the temperature tides at the tropics and solstice the tidal effect is not sufficient to account for the observed temperature changes. In the stratosphere where there is no tidal bias, the

temperature enhancement concurrent with the time of the SSW can still be traced in the MLS and SABER height–time cross-sections.

The spectral analysis applied to the temperature and wind data both for the stratosphere and mesosphere showed very good correlations between the peak of stationary waves with zonal wave number $m = 1$, the enhancement of the westward-propagating planetary waves and the onset of the SSW event. This was most clearly seen in the wavelet results for the 2003–2004 major SSW event. The most pronounced traveling wave in the stratosphere for this period was a westward 7-day $m = 1$ wave, which peaked in late December 2003 in all three fields. A long-period 12–18 day wave preceded the 7-day wave peak.

These results are consistent with the main pattern of stratosphere/mesosphere coupling observed at middle and high latitudes during SSW events and add to the better understanding of the global effects of these SSW on the tropical mesosphere.

Acknowledgements

Portions of this study have been carried out with the support of the INTAS Grant 03-51-6425.

References

Andrews, D.G., Holton, J.R., Leovy, C.B., 1987. Middle Atmosphere Dynamics. Academic Press, London, pp. 259–294.

Baldwin, M.P., Gray, L.J., Dunkerton, T.J., et al., 2001. The quasi-biennial oscillation. Reviews of Geophysics 39, 179–229.

Barath, F.T., et al., 1993. The upper atmosphere research satellite microwave limb sounder instrument. Journal of Geophysical Research 98, 10,751–10,762.

Cho, Y.-M., Shepherd, G.G., Won, Y.-I., Sargoytchev, S., Brown, S., Solheim, S., 2004. MLT cooling during stratospheric warming events. Geophysical Research Letters 31, 0L10104.

Delisi, D.P., Dunkerton, T.J., 1988. Seasonal variation of the semiannual oscillation. Journal of the Atmospheric Sciences 45, 2772–2787.

Fedulina, I.N., Pogoreltsev, A.I., Vaughan, G., 2004. Seasonal, interannual and short-term variability of planetary waves in Met Office stratospheric assimilated fields. Quaternary Journal of the Royal Meteorological Society A 130 (602), 2445–2458.

Forbes, J.M., 1982. Atmospheric tides, 1, Model description and results for the solar diurnal component. Journal of Geophysical Research 87, 5222–5240.

Forbes, J.M., Wu, D., 2006. Solar tides as revealed by measurements of mesospheric temperature by the MLS experiments on UARS. Journal of the Atmospheric Sciences 63 (7), 1776–1797.

Forbes, J.M., Hagan, M.E., Miyahara, S., Vial, F., Manson, A.H., Meek, C.E., Portnyagin, Y.I., 1995. Quasi 16-day oscillation in the mesosphere and lower thermosphere. Journal of Geophysical Research 100 (D5), 9149–9163.

Fritz, S., Soules, S.D., 1970. Large-scale temperature changes in the stratosphere observed from Nimbus III. Journal of the Atmospheric Sciences 27, 1091–1097.

Garcia, R.R., Lieberman, R., Russell III, J.M., Mlynczak, M.G., 2005. Large-scale waves in the mesosphere and lower thermosphere observed by SABER. Journal of the Atmospheric Sciences 62, 4384–4399.

Gordienko, G.I., Fedulina, I.N., Altadill, D., Shepherd, M.G., 2007. The upper ionosphere variability over Alma-Ata and Observatorio del Ebro using the foF2 data obtained during the winter/spring period of 2003–2004. Journal of Atmospheric and Solar-Terrestrial Physics, in press, doi:10.1016/j.jastp.2007.05.008.

Gray, L.J., Phipps, S.J., Dunkerton, T.J., Baldwin, M.P., Drysdale, E.F., Allen, M.R., 2001. A data study of the influence of the equatorial upper stratosphere on northern-hemisphere stratospheric warmings. Quaternary Journal of the Royal Meteorological Society 127, 1985–2003.

Gregory, J.B., Manson, A., 1975. Winds and wave motions to 110 km at mid-latitudes, III, Response of mesospheric and thermospheric winds to major stratospheric warmings. Journal of the Atmospheric Sciences 32, 1676–1681.

Hauchecorne, A., Maillard, A., 1990. A 2-D dynamical model of mesospheric temperature inversions in winter. Geophysical Research Letters 17, 2197–2200.

Hirota, I., Barnett, J., 1977. Planetary waves in the winter mesosphere—preliminary analysis of Nimbus 6 PMR results. Quaternary Journal of the Royal Meteorological Society 103, 487–498.

Hocke, K., 1998. Phase estimation with the Lomb–Scargle periodogram method. Annales de Geophysique 16, 356–358.

Hoffmann, P., Singer, W., Keuer, D., 2002. Variability of the mesospheric wind field at middle and Arctic latitudes in winter and its relation to stratospheric circulation disturbances. Journal of the Atmospheric and Solar-Terrestrial Physics 64, 1229–1240.

Kodera, K., 2006. Influence of stratospheric sudden warming on the equatorial troposphere. Geophysical Research Letters 33, L06804.

Labitzke, K., 1972. Temperature changes in the mesosphere and stratosphere connected with circulation changes in winter. Journal of the Atmospheric Sciences 29, 756–766.

Labitzke, K., 1987. Sunspots, the QBO and the stratospheric temperature in the north polar region. Geophysical Research Letters 14, 535–537.

Leblanc, T., Hauchecorne, A., 1997. Recent observations of mesospheric temperature inversions. Journal of Geophysical Research 102, 19471–19482.

Liu, H.-L., Roble, R.G., 2002. A study of a self-generated stratospheric sudden warming and its mesospheric-lower thermosphereic impacts using the coupled TIME-GCM/CCM3. Journal of Geophysical Research 107 (D23), 4695.

Luo, Y., Manson, A.H., Meek, C.E., Meyer, C.K., Burrage, M.D., Fritts, D.C., Hall, C.M., Hocking, W.K., MacDougall, J., Riggin, D.M., Vincent, R.A., 2002. The 16-day planetary wave: multi-MF radar observations from the arctic to equator

and comparison with the HRDI measurements and the GSWM modelling results. Annales de Geophysique 20, 691–709.

Manney, G.L., Zurek, R.W., Gelman, M.E., Miller, A.J., Nagatani, R., 1994. The anomalous arctic lower stratospheric polar vortex of 1992–1993. Geophysical Research Letters 21 (22), 2405–2408.

Manney, G.L., Kruger, K., Sabutis, J.L., Sena, S.A., Pawson, S., 2005. The remarkable 2003–2004 winter and other recent warm winters in the Arctic stratosphere since the later 1990s. Journal of Geophysical Research 110, D04107.

Manson, A.H., Meek, C., Chshyolkova, T., et al., 2006. Winter warmings, tides and planetary waves: comparisons between CMAM (with interactive chemistry) and MFR-MetO observations and data. Annales de Geophysique 24, 1–26.

Matsuno, T., 1971. A dynamical model of the stratospheric sudden warming. Journal of the Atmospheric Sciences 28, 1479–1494.

Meriwether, J.W., Gerrard, A.J., 2004. Mesosphere inversion layers and stratosphere temperature enhancements. Reviews of Geophysics 42 (1–31), RG3003, (2003RG000133).

Meriwether, J.W., Gao, X., Wickwar, V.B., Wilkerson, T., Beissner, K., Collins, S., Hagan, M.H., 1998. Observed coupling of the mesosphere inversion layer to the thermal tidal structure. Geophysical Research Letters 25 (9), 1479–1482.

Mertens, C.J., Mlynczak, M.G., Lopez-Puertas, M., Wintersteiner, P.P., Picard, R.H., Winick, J.R., Gordley, L.L., Russell III, J.M., 2001. Retrieval of mesospheric and lower thermospheric kinetic temperature from measurements of CO_2 15 μm Earth limb emission under non-LTE conditions. Geophysical Research Letters 28, 1391–1394.

Mertens, C.J., Mlynczak, M.G., Lopez-Puertas, M., Wintersteiner, P.P., Picard, R.H., Winick, J.R., Gordley, L.L., Russell III, J.M., 2002. Retrieval of the kinetic temperature and carbon dioxide abundance from non-local thermodynamic equilibrium limb emission measurements made by the SABER experiment on the TIMED satellite. In: Proceedings of the SPIE, Remote Sensing of Clouds and the Atmosphere VII, Agia, Greece, pp. 162–171.

Mirabø, H.K., Deehr, C.S., Lybekk, B., 1984. Polar cap OH airglow rotational temperatures in the mesopause during a stratospheric warming event. Planetary and Space Science 32, 853–856.

Mlynczak, M.G., 1997. Energetics of the mesosphere and lower thermosphere and the SABER experiment. Advances in Space Research 20, 1177–1183.

Mukherjee, B.K., Ramana Murty, Bh.V., 1972. High-level warmings over a tropical station. Monthly Weather Review 100 (9), 674–681.

Mukherjee, B.K., Indira, K., Dani, K.K., 1987. Perturbations in tropical middle atmosphere during winter, 1984–1985. Meteorology and Atmospheric Physics 37, 17–26.

Naujokat, B., Labitzke, K., Lenschow, R., Rajewski, B., Wiesner, M., Wohlfahrt, C.-R., 1994. The stratospheric winter 1993/1994: a winter with some minor warmings and an early final warming. Beilage zur berliner Wetterkarte 81/94, SO, 24/94.

Orsolini, Y.J., Limpasuvan, V., Leovy, C., 1997. The tropical stratopause in the UKMO stratospheric analyses: evidence for a 2-day wave and inertial circulation. Quaternary Journal of the Royal Meteorological Society 123, 1707–1724.

Pancheva, D., Mukhtarov, P., 2000. Wavelet analysis on transient behaviour of tidal amplitude fluctuations observed by meteor radar in the lower thermosphere above Bulgaria. Annales de Geophysique 18 (3), 316–331.

Quiroz, R.S., 1969. The warming of the upper stratosphere in February 1966 and the associated structure of the mesosphere. Monthly Weather Review 97 (8), 541–552.

Rajaram, R., Gurubaran, S., 1998. Seasonal variabilities of low-latitude mesospheric winds. Annales de Geophysique 16, 197–204.

Reber, C.A., Trevathan, E.C., O'Neal, J.R., Luther, R.M., 1993. Upper Atmosphere Research Satellite (UARS) mission. Journal of Geophysical Research 98, 10,643–10,647.

Russell III, J.M., Mlynczak, M.G., Goldley, L.L., Tansock, J., Espin, R., 1999. An overview of the SABER experiment and preliminary calibration results. Proceedings of SPIE 3756, 277–288.

Salby, M.L., 1981. Rossby normal modes in nonuniform background configuration. Part II: equinox and solstice conditions. Journal of the Atmospheric Sciences 38, 1837–1840.

Sassi, F., Garcia, R.R., Boville, B.A., Liu, H., 2002. On temperature inversions and the mesospheric surf zone. Journal of Geophysical Research 107, 4380.

Scargle, J.D., 1982. Studies in aeronomical time series analysis: II. Statistical aspects of spectral analysis of unevenly spaced data. Astrophysics Journal 263, 835–853.

Shepherd, G.G., Thuillier, G., Gault, W.A., et al., 1993. WINDII, the wind imaging interferometer on the Upper Atmosphere Research satellite. Journal of Geophysical Research 98, 10725–10750.

Shepherd, M.G., Reid, B., Zhang, S.P., Solheim, B.H., Shepherd, G.G., Wickwar, V.B., Herron, J.P., 2001. Retrieval and validation of mesospheric temperatures from Wind Imaging Interferometer observations. Journal of Geophysical Research 106, 24,813–24,829.

Shepherd, M.G., Evans, W.J.F., Hernandez, G., Offermann, D., Takahashi, H., 2004. Global variability of mesospheric temperature: mean temperature field. Journal of Geophysical Research, D 109 (D24), D24117.

Shepherd, M.G., Shepherd, G.G., Evans, W.F.J., Sridharan, S., 2005. Global variability of mesospheric temperature: planetary scale perturbations at equatorial and tropical latitudes. Journal of Geophysical Research 110 (D24), D24103.

Shepherd, M.G., Wu, D.L., Gurubaran, S., Fedulina, I.N., 2007. Temperature variability in the tropical mesosphere during the northern hemisphere Winter. Advances in Space Research, in press, doi:10.1016/j/asr.2007.04.035.

Sivakumar, V., Morel, B., Bencherif, H., Baray, J.L., Baldy, S., Hauchecorne, A., Rao, P.B., 2004. Rayleigh lidar observation of a warm stratopause over a tropical site, Gadanki (13.5°N, 79.2°E). Atmospheric Chemistry and Physics 4, 1989–1996.

Smith, A.S., 1985. Wave transience and wave-mean flow interaction caused by the interference of stationary and travelling waves. Journal of the Atmospheric Sciences 42 (6), 529–535.

Smith, A.K., 1996. Longitudinal variations in mesospheric winds: evidence for gravity wave filtering by planetary waves. Journal of the Atmospheric Sciences 53, 1156–1173.

Smith, A.K., 1997. Stationary planetary waves in upper mesospheric winds. Journal of the Atmospheric Sciences 54, 2129–2145.

Sridharan, S., Gurubaran, S., Rajaram, R., 2003. QBO influence on the variability of planetary waves in the equatorial mesopause region. Earth Planets Space 55, 687–696.

Swinbank, R., O'Neill, A., 1994a. A stratosphere–troposphere data assimilation system. Monthly Weather Review 122, 686–702.

Swinbank, R., O'Neill, A., 1994b. Quasi-biennial and semi-annual oscillations in equatorial wind fields constructed by data assimilation. Geophysical Research Letters 21, 2099–2102.

Swinbank, R., Ortland, D.A., 2003. Compilation of wind data for the Upper Atmosphere Research Satellite (UARS) Reference Atmosphere Project. Journal of Geophysical Research 108 (D19), 4615.

Talaat, E.R., Yee, J.-H., Zhu, Xun, 2001. Observations of the 6.5-day wave in the mesosphere and lower stratosphere. Journal of Geophysical Research 106, 20715–20723.

Torrence, Ch., Compo, G.P., 1998. A practical guide to wavelet analysis. Bulletin of the American Meteorological Society 79 (1), 61–78.

Venne, D.E., Dartt, D.G., Rodgers, C.D., 1988. A stationary planetary-scale feature in the tropical mesopause temperature field. Geophysical Research Letters 15 (10), 1129–1132.

Vincent, R.A., Lesicar, D., 1991. Dynamics of the equatorial mesosphere: first results with a new generation partial reflection radar. Geophysical Research Letters, 18,825–18,828.

Walterscheid, R.L., Sivjee, G.G., Roble, R.G., 2000. Mesospheric and lower thermospheric manifestations of a stratospheric warming event over Eureka, Canada (80°N). Geophysical Research Letters 27 (18), 2897–2900.

Wang, D.Y., Ward, W.E., Shepherd, G.G., et al., 2000. Stationary planetary waves inferred from WINDII wind data taken within altitudes 90–120 km during 1991–96. Journal of the Atmospheric Sciences 57 (12), 1906–1918.

Whiteway, J.A., Carswell, A.I., 1994. Rayleigh lidar observations of thermal structure and gravity wave activity in the high arctic during a stratospheric warming. Journal of the Atmospheric Sciences 51, 3122–3136.

Wu, D.L., Hays, P.B., Skinner, W.R., 1994. Observations of the 5-day wave in the mesosphere and lower thermosphere. Geophysical Research Letters 21 (24), 2733–2736.

Wu, D.L., Read, W.G., Shippony, Z., Leblanc, T., Duck, T.J., Ortland, D.A., Sica, R.J., Argall, P.S., Oberheide, J., Hauchecorne, A., Keckhut, P., She, C.Y., Krueger, D.A., 2003. Mesospheric temperature from UARS MLS: retrieval and validation. Journal of Atmospheric and Solar-Terrestrial Physics 65, 245–267.

Yee, J.H., 2003. TIMED mission science overview. John Hopkins APL Technical Digest 24 (2), 136–141 Apr–Jun.